

1 **Wild Patagonian yeast improve the evolutionary potential of novel interspecific hybrid**  
2 **strains for Lager brewing**

3

4 Jennifer Molinet<sup>1,2,3\*</sup>, Juan P. Navarrete<sup>1</sup>, Carlos A. Villarroel<sup>1,4</sup>, Pablo Villarreal<sup>1,2</sup>, Felipe I.  
5 Sandoval<sup>1</sup>, Roberto F. Nespolo<sup>1,5,6,7</sup>, Rike Stelkens<sup>3</sup> and Francisco A. Cubillos<sup>1,2,5\*</sup>.

6

7 <sup>1</sup>ANID-Millennium Science Initiative-Millennium Institute for Integrative Biology (iBio),  
8 Santiago, Chile.

9 <sup>2</sup>Departamento de Biología, Facultad de Química y Biología, Universidad de Santiago de  
10 Chile, Santiago, Chile.

11 <sup>3</sup>Department of Zoology, Stockholm University, Stockholm, Sweden.

12 <sup>4</sup>Centro de Biotecnología de los Recursos Naturales (CENBio), Facultad de Ciencias  
13 Agrarias y Forestales, Universidad Católica del Maule, Talca, Chile.

14 <sup>5</sup>ANID-Millennium Nucleus of Patagonian Limit of Life (LiLi), Valdivia, Chile.

15 <sup>6</sup>Instituto de Ciencias Ambientales y Evolutivas, Facultad de Ciencias, Universidad Austral  
16 de Chile, Valdivia, Chile.

17 <sup>7</sup>Center of Applied Ecology and Sustainability (CAPES), Santiago, Chile.

18 \* Address correspondence to Francisco A. Cubillos, [francisco.cubillos.r@usach.cl](mailto:francisco.cubillos.r@usach.cl) and  
19 Jennifer Molinet, [jennifer.molinet@usach.cl](mailto:jennifer.molinet@usach.cl)

20

21 **ABSTRACT**

22 Lager yeasts are limited to a few strains worldwide, imposing restrictions on flavour and  
23 aroma diversity and hindering our understanding of the complex evolutionary mechanisms  
24 during yeast domestication. The recent finding of diverse *S. eubayanus* lineages from  
25 Patagonia offers potential for generating new Lager yeasts and obtaining insights into the  
26 domestication process. Here, we leverage the natural genetic diversity of *S. eubayanus* and  
27 expand the Lager yeast repertoire by including three distinct Patagonian *S. eubayanus*  
28 lineages. We used experimental evolution and selection on desirable traits to enhance the  
29 fermentation profiles of novel *S. cerevisiae* x *S. eubayanus* hybrids. Our analyses reveal an  
30 intricate interplay of pre-existing diversity, selection on species-specific mitochondria, *de-*  
31 *novo* mutations, and gene copy variations in sugar metabolism genes, resulting in high  
32 ethanol production and unique aroma profiles. Hybrids with *S. eubayanus* mitochondria  
33 exhibited greater evolutionary potential and superior fitness post-evolution, analogous to  
34 commercial Lager hybrids. Using genome-wide screens of the parental subgenomes, we  
35 identified genetic changes in *IRA2*, *SNF3*, *IMA1* and *MALX* genes that influence maltose  
36 metabolism, and increase glycolytic flux and sugar consumption in the evolved hybrids.  
37 Functional validation and transcriptome analyses confirmed increased maltose-related gene  
38 expression, influencing greater maltotriose consumption in evolved hybrids. This study  
39 demonstrates the potential for generating industrially viable Lager yeast hybrids from wild  
40 Patagonian strains. Our hybridization, evolution, and mitochondrial selection approach  
41 produced hybrids with high fermentation capacity, expands Lager beer brewing options, and  
42 deepens our knowledge of Lager yeast domestication.

43

44 Keywords: Interspecific hybrids, *S. cerevisiae*, *S. eubayanus*, lager beer, experimental  
45 evolution.

## 46 INTRODUCTION

47 Humans have paved the way for microbes, such as yeast, to evolve desirable features for  
48 making bread, wine, beer and many other fermented beverages for millennia (Steensels et  
49 al., 2019). The fermentation environment, characterized by limited oxygen, high ethanol  
50 concentrations, and microbial competition for nutrients (typically yeasts, molds, and  
51 bacteria) can be considered stressful (Walker & Basso, 2019). One evolutionary mechanism  
52 to overcome harsh conditions is hybridization, because it rapidly combines beneficial  
53 phenotypic features of distantly related species and generates large amounts of genetic  
54 variation available for natural selection to act on (Abbott et al., 2013; Steensels et al., 2021;  
55 R. Stelkens & Bendixsen, 2022). Hybrids can also express unique phenotypic traits not seen  
56 in the parental populations through the recombination of parental genetic material, enabling  
57 them to thrive in different ecological niches (Rieseberg et al., 2003; Steensels et al., 2021; R.  
58 B. Stelkens et al., 2014; R. Stelkens & Seehausen, 2009). An iconic example is the  
59 domestication of the hybrid yeast *Saccharomyces pastorianus* to produce modern lager  
60 (pilsner) beers. *S. pastorianus* is the result of the successful interspecies hybridization  
61 between *S. cerevisiae* and *S. eubayanus* (Gallone et al., 2019; Langdon et al., 2019). Hybrids  
62 have been shown to benefit from the cold tolerance of *S. eubayanus* and the superior  
63 fermentation kinetics of *S. cerevisiae* (Gibson et al., 2017). We now know that domestication  
64 over the last 500 years has generated Lager yeast strains with the unique ability to rapidly  
65 ferment at lower temperatures resulting in a crisp flavour profile and efficient sedimentation,  
66 improving the clarity of the final product. However, the genetic diversity of commercial  
67 Lager yeast strains is extremely limited, mainly due to the standardization of industrial Lager  
68 production during the nineteenth century in Germany (Gallone et al., 2019; Hutzler et al.,  
69 2023). This gave rise to only two genetically distinct *S. pastorianus* subgroups, Group 1

70 strains ('Saaz') and Group 2 strains ('Frohberg'). The poor genetic diversity of Lager strains  
71 used in commercial brewing today (85 Lager strains commercially available versus 358 Ale  
72 strains (Bonatto, 2021)) puts tight constraints on the variety of flavours and aromas found in  
73 Lager beer. At the same time, it limits our understanding of the evolutionary mechanism  
74 operating during the yeast domestication process.

75         The discovery of *S. eubayanus* in Patagonia in 2011 (Libkind et al., 2011), opened  
76 new possibilities for creating novel hybrid strains by using the full range of natural genetic  
77 diversity found in this species. It also provides an opportunity to better understand the lager  
78 yeast domestication process. Phylogenetic analyses have revealed six distinct lineages of *S.*  
79 *eubayanus*, including China, Patagonia A ('PA'), Holarctic, and Patagonia B, 'PB-1', 'PB-  
80 2' and 'PB-3', and some admixed strains derived from ancient crosses (Langdon et al., 2020;  
81 Nespolo et al., 2020). Of these, *S. eubayanus* from Patagonia displays the broadest  
82 phenotypic diversity for a wide range of traits, including high maltose consumption, aroma  
83 profiles and fermentation capacity (Mardones et al., 2020; Nespolo et al., 2020; Urbina et al.,  
84 2020). The distinctive traits of wild Patagonian *S. eubayanus* strains indicate their potential  
85 for crafting new Lager beer styles. These strains could yield novel taste and aroma profiles,  
86 approaching similar complexity and diversity in flavour, appearance, and mouthfeel as Ale  
87 beers.

88         Lager yeast hybrids experienced an intense domestication process through selection  
89 and re-pitching during beer fermentation since the 17<sup>th</sup> century (Gallone et al., 2019; Gorter  
90 De Vries, Pronk, et al., 2019; Hutzler et al., 2023; Langdon et al., 2019; Okuno et al., 2015),  
91 a process similar to experimental evolution (Gibson et al., 2020; Gorter De Vries, Voskamp,  
92 et al., 2019). Experimental evolution with microbes is a powerful tool to study adaptive  
93 responses to selection under environmental constraints (Barrick & Lenski, 2013; Cooper,

94 2018; Maddamsetti et al., 2015; Payen & Dunham, 2016). Recent studies on novel *S.*  
95 *cerevisiae* x *S. eubayanus* hybrids suggest that hybrid fermentative vigour at low temperature  
96 results from a variety of genetic changes, including loss of heterozygosity (LOH), ectopic  
97 recombination, transcriptional rewiring, selection of superior parental alleles (Sipiczki,  
98 2018), heterozygote advantage due to the complementation of loss-of-function mutations in  
99 the F1 hybrid genome (Brouwers et al., 2019), and novel structural and single nucleotide  
100 variants in the hybrid genome (Krogerus, Holmström, et al., 2018). A recent transcriptome  
101 analyses of a laboratory-made Lager hybrid strain under fermentation conditions highlighted  
102 that the regulatory ‘cross-talk’ between the parental subgenomes caused a novel sugar  
103 consumption phenotype in the hybrid (maltotriose utilization, essential for Lager  
104 fermentation), which was absent in both parental strains (Brouwers et al., 2019). Although  
105 these studies have greatly contributed to our understanding of the genetic basis of different  
106 lager phenotypes, most studies only considered a single *S. eubayanus* genetic background  
107 (type strain CBS 12357), which alone is not representative of the species-rich genetic  
108 diversity.

109         Here, we hybridized three different *S. cerevisiae* and *S. eubayanus* strains to generate  
110 genetically and phenotypically diverse novel Lager hybrids via spore-to-spore mating. The  
111 initial *de novo* hybrids had fermentation capacities comparable to those of their parental  
112 strains and did not show positive heterosis. However, when we subjected hybrids to a ‘fast  
113 motion’ improvement process using experimental evolution under different fermentation  
114 conditions for 250 generations, they exceeded the fitness of the ancestral hybrids, particularly  
115 those retaining the *S. eubayanus* mitochondria. Superior hybrid fitness was explained by  
116 faster fermentation performance and greater maltose and maltotriose consumption We found  
117 that copy number variation in *MAL* genes in the *S. cerevisiae* subgenome, together with SNPs

118 in genes related to glycolytic flux, induced significantly greater expression levels of *MAL*  
119 and *IMA1* genes, and led to improved fitness under fermentative conditions in these novel *S.*  
120 *cerevisiae* x *S. eubayanus* yeast hybrids. Furthermore, evolved hybrids had significantly  
121 distinct aroma profiles, varying significantly from the established profiles found in lager beer.

122

## 123 **MATERIALS AND METHODS**

### 124 **Parental strains**

125 Three *S. cerevisiae* strains were selected for hybridization from a collection of 15 strains  
126 isolated from different wine-producing areas in Central Chile and previously described by  
127 (Martinez et al., 2004). Similarly, three *S. eubayanus* parental strains were selected from a  
128 collection of strains isolated from different locations in Chilean Patagonia, exhibiting high  
129 fermentative capacity and representative of the different Patagonia-B lineages (PB-1, PB-2  
130 and PB-3) (Nespolo et al., 2020). The *S. pastorianus* Saflager W34/70 (Fermentis, France)  
131 strain was used as a commercial Lager fermentation control. All strains were maintained in  
132 YPD agar (1% yeast extract, 2% peptone, 2% glucose and 2 % agar) and stored at -80 °C in  
133 20% glycerol stocks. Strains are listed in **Table S1A**.

### 134 **Interspecific hybrids strains and mitochondria genotyping**

135 Parental strains were sporulated on 2% potassium acetate agar plates (2% agar) for at least  
136 seven days at 20 °C. Interspecific F1 hybrids were generated through spore-spore mating  
137 between *S. eubayanus* strains and *S. cerevisiae* strains (**Figure S1**). For this, tetrads were  
138 treated with 10 µL Zymolyase 100 T (50 mg/mL) and spores of opposite species were  
139 dissected and placed next to each other on a YPD agar plates using a SporePlay

140 micromanipulator (Singer Instruments, UK). Plates were incubated at two different  
141 temperatures, 12 and 20 °C, for 2-5 days to preserve the cold- and heat-tolerant mitochondria,  
142 respectively, as previously described (Baker et al., 2019; Hewitt et al., 2020), resulting in  
143 nine different F1 hybrids (ranging from H1 until H9, **Table S1A**). This procedure was  
144 repeated on 25 tetrads of each species, for each type of cross (H1 to H9) and temperature (12  
145 and 20 °C), resulting in 18 different cross x temperature combinations. Finally, colonies were  
146 isolated, re-streaked on fresh YPD agar plates, and continued to be incubated at 12 and 20  
147 °C. The hybrid status of isolated colonies was confirmed by amplification of rDNA-PCR  
148 (ITS1, 5.8S and ITS2) using universal fungal primers ITS1 and ITS4 (Esteve-Zarzoso et al.,  
149 1999), followed by digestion of the amplicon using the *Hae*III restriction enzyme (Promega,  
150 USA) as previously described (Krogerus et al., 2016) on one colony for each cross attempt  
151 (**Figure S1**). Confirmed F1 hybrids were designated as H1 to H9 based on parental strains,  
152 followed by the hybridization temperature (12 or 20) and the colony number (i.e. H1.20-1  
153 depicts cross 1 at 20 °C (**Table S1A**)). We identified the mitochondrial genotype by Sanger  
154 sequencing the mitochondrial *COX3* gene as previously described (Hewitt et al., 2020).

### 155 **Beer wort fermentation and metabolite screening**

156 Fermentations were carried out in three biological replicates using previously oxygenated  
157 (15 mg/L) 12 °P wort, supplemented with 0.3 ppm ZnCl<sub>2</sub> as previously described (Mardones  
158 et al., 2020). Briefly, pre-cultures were grown in 5 mL 6 °P wort for 24 h at 20 °C with  
159 constant agitation at 150 rpm. Cells were then transferred to 50 mL 12 °P wort and incubated  
160 for 24 h at 20 °C with constant agitation at 150 rpm. Cells were collected by centrifugation  
161 and used to calculate the final cell concentration to inoculate the subsequent fermentation  
162 according to the formula described by (White & Zainasheff, 2010). Cells were inoculated



163 into 50 mL 12 °P wort in 250 mL bottles covered by airlocks containing 30% glycerol. The  
164 fermentations were incubated at 12 or 20 °C, with no agitation for 15 days and monitored by  
165 weighing the bottles daily to determine weight loss over time.

166 Sugar (glucose, fructose, maltose and maltotriose) consumption and ethanol production were  
167 determined by High-Performance Liquid Chromatography (HPLC) after 14 days of  
168 fermentation. Filtered samples (20 µL) were injected in a Shimadzu Prominence HPLC  
169 (Shimadzu, USA) with a BioRad HPX-87H column using 5 mM sulfuric acid and 4 mL  
170 acetonitrile per liter of sulfuric acid as the mobile phase at a 0.5 mL/min flow rate. Volatile  
171 compound production was determined by using HeadSpace Solid-Phase MicroExtraction  
172 followed by Gas Chromatography-Mass Spectrometry (HS-SPME-GC/MS) after 14 days of  
173 fermentation as previously described (Urbina et al., 2020).

#### 174 **Phenotypic characterization**

175 Hybrids and parental strains were phenotypically characterized under microculture  
176 conditions as previously described (Molinet, Urbina, et al., 2022). Briefly, we estimated  
177 mitotic growth in 96-well plates containing Yeast Nitrogen Base (YNB) supplemented with  
178 2% glucose, 2% maltose, 2% maltotriose, 2% glucose and 9% ethanol, 2% glucose and 10%  
179 sorbitol, and under carbon source switching from glucose to maltose as previously described  
180 (Molinet, Eizaguirre, et al., 2022). All conditions were evaluated at 25 °C. Lag phase, growth  
181 efficiency and the maximum specific growth rate were determined as previously described  
182 (Ibstedt et al., 2015; Warringer & Blomberg, 2003). For this, the parameters were calculated  
183 following curve fitting (OD values were transformed to ln) using the Gompertz function  
184 (Zwietering M et al., 1990) in R (version 4.03).

185 Mid-parent and best-parent heterosis were determined as previously described (Bernardes et  
186 al., 2017; Steensels et al., 2014), using equation 1 and 2, where mid-parent heterosis denotes  
187 the hybrid deviation from the mid-parent performance and best-parent heterosis denotes the  
188 hybrid deviation from the better parent phenotypic value (Zörgö et al., 2012).

$$189 \quad \text{Mid-parent heterosis} = \frac{\text{Phenotypic value}_h}{\text{Phenotypic value}_p} \quad (1)$$

$$190 \quad \text{Best-parent heterosis} = \frac{\text{Phenotypic value}_h}{\text{Phenotypic value}_{bp}} \quad (2)$$

191 Where:

$$192 \quad \text{Phenotypic value}_h = \text{phenotypic value}_{\text{hybrid}}$$

$$193 \quad \text{Phenotypic value}_p = \frac{\text{phenotypic value}_{\text{parental1}} + \text{phenotypic value}_{\text{parental2}}}{2}$$

$$194 \quad \text{Phenotypic value}_{bp} = \max(\text{phenotypic value}_{\text{parental1}}, \text{phenotypic value}_{\text{parental2}})$$

## 195 **Experimental evolution**

196 Experimental evolution was carried out at 20°C under two different media conditions (M and  
197 T): 1) YNB + 2% maltose supplemented with 9% ethanol (M) and 2) YNB + 1% maltose +  
198 1% maltotriose supplemented with 9% ethanol (T). Experimental evolution assays in maltose  
199 were performed in a final volume of 1 mL in 2 mL tubes, while those in maltose and  
200 maltotriose were performed in a 96-well plate under a final volume of 200 µL. Each hybrid  
201 strain was first grown in 0.67% YNB medium with 2% maltose at 25 °C for 24 h with  
202 constant agitation at 150 rpm. Each pre-inoculum was then used to inoculate each evolution  
203 line at an initial OD<sub>600nm</sub> of 0.1, with three replicate lines per strain in medium M and four

204 replicate lines in medium T. Lines in medium M were incubated at 20 °C for 72 h. Lines in  
205 medium T were incubated for 144 h at 20 °C. After this, cultures were then serially  
206 transferred into fresh medium for an initial OD<sub>600nm</sub> of 0.1. Serial transfers were repeated for  
207 250 generations in total (approximately seven months). The number of generations was  
208 determined using the formula  $\log(\text{final cells} - \text{initial cells})/\log_2$  (Mardones et al., 2021).  
209 Population samples were stored at -80 °C in 20% glycerol stocks after 50, 100, 150, 200 and  
210 250 generations. After 250 generations, three colonies were isolated for each replicate line  
211 on YPM solid medium (1% yeast extract, 2% peptone, 2% maltose and 2 % agar)  
212 supplemented with 6% ethanol. The fastest growing colonies were stored at -80 °C in 20%  
213 glycerol stocks. The fitness increase of each the 28 evolved line was determined as the ratio  
214 between the phenotypic value of a given line and the equivalent of its respective ancestral  
215 hybrid.

## 216 **Genomic characterization**

217 Genomic DNA was obtained for whole-genome sequencing using the YeaStar Genomic  
218 DNA Kit (Zymo Research, USA) and sequenced in an Illumina NextSeq500 following the  
219 manufacturer's instructions. Variant calling and filtering were done with GATK version  
220 4.3.0.0 (Depristo et al., 2011). Briefly, cleaned reads were mapped to a concatenated  
221 reference genome consisting of *S. cerevisiae* strain DBVPG6765 (Yue et al., 2017) and *S.*  
222 *eubayanus* strain CL216.1 (Mardones et al., 2020) using BWA mem 0.7.17 (Li & Durbin,  
223 2010), after which output bam files were sorted and indexed using Samtools 1.13 (Li et al.,  
224 2009). Variants were called per sample using HaplotypeCaller (default settings) generating  
225 g.vcf files. Variant databases were built using GenomicsDBImport and genotypes were  
226 called using GenotypeGVCFs (-G StandardAnnotation). SNPs and INDELS were extracted

227 and filtered out separately using SelectVariants. We then applied recommended filters with  
228 the following options: QD < 2.0, FS > 60.0, MQ < 40.0, SOR > 4.0, MQRankSum < -12.5,  
229 ReadPosRankSum < -8.0. This vcf file was further filtered removing missing data using the  
230 option `-max-missing 1`, filtering out sites with a coverage below 5<sup>th</sup> or above the 95<sup>th</sup>  
231 coverage sample percentile using the options `-min-meanDP` and `-max-meanDP`, and  
232 minimum site quality of 30 (`--minQ 30`) in vcftools 0.1.16 (Danecek et al., 2011). Sites with  
233 a mappability less than 1 calculated by GenMap 1.3.0 (Pockrandt et al., 2020) were filtered  
234 using bedtools 2.18 (Quinlan & Hall, 2010). As an additional filtering step, the ancestral and  
235 evolved vcf files were intersected using BCFtools 1.3.1 (Danecek et al., 2021) and variants  
236 with shared positions were extracted from the vcf files of the evolved hybrids. Annotation  
237 and effect prediction of the variants were performed with SnpEff (Cingolani et al., 2012).

238 We used sppIDer (Langdon et al., 2018) to assess the proportional genomic contribution of  
239 each species to the nuclear and mitochondrial genomes in each sequenced hybrid. In addition,  
240 we used the tool to identify potential aneuploidies within these genomes. CNVs were called  
241 using CNVkit (`--method wgs, -target-avg-size 1000`) (Talevich et al., 2016). As the analysis  
242 was performed on a haploid reference (both parental genomes were present), a CNV of  $\log_2$   
243 = 1 corresponds to a duplication.

#### 244 **RNA-seq analysis**

245 Gene expression analysis was performed on ancestral and evolved hybrid strains H3-A and  
246 H3-E. RNA was obtained and processed after 24 h under beer wort fermentation in triplicates,  
247 using the E.Z.N.A Total RNA kit I (OMEGA) as previously described (Molinet, Eizaguirre,  
248 et al., 2022; Venegas et al., 2023). Total RNA was recovered using the RNA Clean and

249 Concentrator Kit (Zymo Research). RNA integrity was confirmed using a Fragment Analyzer  
250 (Agilent). Illumina sequencing was performed in NextSeq500 platform.

251 Reads quality was evaluated using the fastqc tool  
252 (<https://www.bioinformatics.babraham.ac.uk/projects/fastqc/>) and processed using fastp (-3  
253 140) (Chen et al., 2018). Reads were mapped to a concatenated fasta file of the DBVPG6765  
254 and CL216.1 genome sequences. To account for mapping bias due to the different genetic  
255 distances of the parental strains to their reference strains, the L3 and CL710.1 parental strains  
256 were re-sequenced using WGS, after which genomic reads were mapped with BWA (Li &  
257 Durbin, 2010) to the DBVPG6765 and CL216 references and SNPs were called using  
258 freebayes (Garrison & Marth, 2012). These SNPs were used to correct the hybrid genome  
259 sequence using the GATK FastaAlternateReferenceMaker tool. RNAseq reads were mapped  
260 to this hybrid reference using STAR (-outSAMmultNmax 1, -outMultimapperOrder random)  
261 (Dobin et al., 2013). Counts were obtained with featureCounts using a concatenated  
262 annotation file (Liao et al., 2014). Counts were further analyzed in R using the DESeq package  
263 (Love et al., 2014). A PCA analysis to evaluate the reproducibility of replicates was  
264 performed, after which two outlier replicates (H3-A replicate 3 and H3-E replicate 2) were  
265 removed. To analyze differences in allele expression, a list of 1-to-1 orthologous genes  
266 between both parental strains were identified using OMA (Zahn-Zabal et al., 2020).  
267 Orthologous genes that differ more than 5% on their gene lengths were excluded. The  
268 differential allelic expression of these orthologous genes was determined using design =  
269 ~parental, with parental being “L3” or “CL710”. Furthermore, orthologous genes that  
270 showed differential allele expression depending on the ancestral or evolved strain  
271 background were assessed using an interaction term (~ parental:condition), with condition

272 being “ancestral” or “evolved”. Finally, to evaluate differences between ancestral and  
273 evolved hybrid strains, all 11,047 hybrid genes (5,508 *S. eubayanus* and 5,539 *S. cerevisiae*)  
274 were individually tested for differential expression using DESeq2. Overall gene expression  
275 differences were evaluated using the design ~condition. For all analyzes an FDR < 0.05 was  
276 used to consider statistical differences. GO term enrichment analyzes on differentially  
277 expressed genes were calculated using the package TOPGO (Alexa & Rahnenfuhrer, 2023).

### 278 ***IRA2* gene validation**

279 The *S. cerevisiae IRA2* polymorphism was validated by Sanger sequencing. PCR products  
280 were purified and sequenced by KIGene, Karolinska Institutet (Sweden). The presence of the  
281 SNP in the evolved hybrid strains was checked by visual inspection of the electropherograms.  
282 Null mutants for the *IRA2* gene in the *S. cerevisiae* sub-genome were generated using  
283 CRISPR-Cas9 (Dicarlo et al., 2013) as previously described (Molinet, Urbina, et al., 2022).  
284 Briefly, the gRNAs were designed using the Benchling online tool  
285 (<https://www.benchling.com/>) and cloned into the pAEF5 plasmid (Fleiss et al., 2019), using  
286 standard “Golden Gate Assembly” (Horwitz et al., 2015). Ancestral and evolved hybrids  
287 were co-transformed with the pAEF5 plasmid carrying the gRNA and the Cas9 gene, together  
288 with a double-stranded DNA fragment (donor DNA). The donor DNA contained  
289 nourseothricin (NAT) resistance cassette, obtained from the pAG25 plasmid (Addgene  
290 plasmid #35121), flanked with sequences of the target allele, corresponding to 50-pb  
291 upstream of start codon and 50-pb downstream of the stop codon. Correct gene deletion was  
292 confirmed by standard colony PCR. All primers, gRNAs, and donor DNA are listed in **Table**  
293 **S1B**.

## 294 **Statistical analysis**

295 Data visualization and statistical analyses were performed with R software version 4.03.  
296 Maximum specific growth rates and total CO<sub>2</sub> loss were compared using an analysis of  
297 variance (ANOVA) and differences between the mean values of three replicates were tested  
298 using Student's t-test and corrected for multiple comparisons using the Benjamini-Hochberg  
299 method. A *p-value* less than 0.05 ( $p < 0.05$ ) was considered statistically significant. Heatmaps  
300 were generated using the ComplexHeatmap package version 2.6.2. A principal component  
301 analysis (PCA) was performed on phenotypic data using the FactoMineR package version  
302 2.4 and the factoextra package version 1.07 for extracting, visualizing and interpreting the  
303 results.

## 304 **Data availability**

305 All fastq sequences were deposited in the National Center for Biotechnology Information  
306 (NCBI) as a Sequence Read Archive under the BioProject accession number PRJNA1043100  
307 (<http://www.ncbi.nlm.nih.gov/bioproject/1043100>).

## 308 **RESULTS**

309 ***De novo S. cerevisiae* x *S. eubayanus* F1 hybrids show similar phenotypes as their**  
310 **parental strains.**

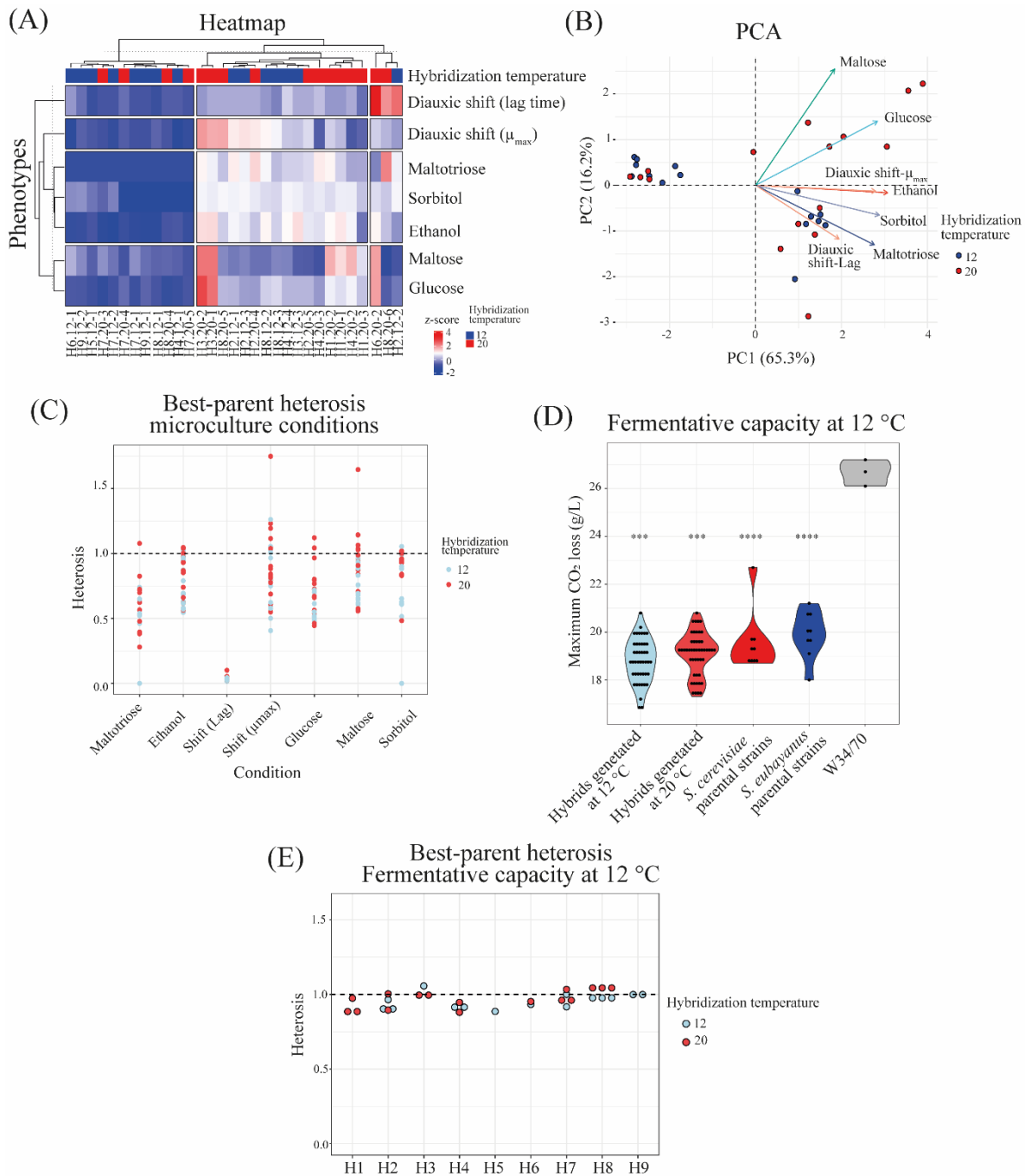
311 The *S. cerevisiae* and *S. eubayanus* parental strains were selected from a previously described  
312 collection of Chilean isolates by (Martinez et al., 2004) and (Nespolo et al., 2020),  
313 respectively (**Table S1A**). Initially, three *S. cerevisiae* strains from vineyards were selected  
314 because they showed: i) the highest maximum CO<sub>2</sub> loss in beer wort (**Figure S2A, Table**

315 **S2**), ii) the best growth performance under maltotriose conditions (**Figure S2B**), and iii) the  
316 most efficient maltotriose uptake during microculture conditions (**Figure S2C**). These strains  
317 were L3, L270, and L348. The selection of *S. eubayanus* parental strains was determined by  
318 two criteria: i) to represent distinct lineages found in the Chilean Patagonia to maximize  
319 genetic diversity (one strain per lineage, PB-1, PB-2, and PB-3), and ii) to display the highest  
320 CO<sub>2</sub> loss during fermentation when compared to strains within their respective lineages based  
321 on previous assays (Nespolo et al., 2020). In this way, we selected CL450.1, CL710.1 and  
322 CL216.1, from PB-1, PB-2, and PB-3, respectively.

323 We first assessed sporulation efficiency and spore viability in the six chosen parental strains  
324 (**Table S2C**). Sporulation efficiency ranged from 12.7% to 95.5% and spore viability ranged  
325 from 15% to 100% across strains. Then, nine different interspecific F1 hybrid crosses were  
326 created by mating three *S. cerevisiae* and three *S. eubayanus* strains through spore-to-spore  
327 mating (**Figure S1**). Mating was conducted at 12 °C and 20 °C to promote the preservation  
328 of the cold- and heat-tolerant mitochondria, respectively, as previously described (Baker et  
329 al., 2019; Hewitt et al., 2020). We obtained 31 interspecific hybrids (**Table S1A**), which we  
330 phenotyped individually under microculture conditions. In this way, we estimated microbial  
331 growth under similar conditions to those encountered during beer wort fermentation, such as  
332 glucose, maltose, maltotriose and ethanol (**Table S3**). Hierarchical clustering of the  
333 phenotypic data denotes three main clusters, where there was no discernible clustering of  
334 hybrids based on their parental strains or hybridization temperature, highlighting the  
335 considerable phenotypic diversity resulting from hybridization (**Figure 1A**). To describe the  
336 phenotypic landscape of the 31 hybrids more comprehensively, we conducted a PCA analysis  
337 (**Figure 1B**). The individual factor map shows that hybrids made at 20°C fall into the right



338 upper quarter of the phenotype space, and are associated with higher growth rate in media  
 339 with maltose and glucose compared to hybrids made at 12 °C. This was particularly the case  
 340 for four hybrid strains (H1, H3, H4 and H6), involving parental strains L3, L270, CL216.1  
 341 and CL710.1 (all p-values < 0.05, one-way ANOVA, **Table S3B**).



342

343 **Figure 1. Phenotypic characterization of interspecific F1 hybrids.** A) Hierarchically  
344 clustered heatmap of phenotypic diversity of 31 interspecific hybrids strains under  
345 microculture conditions. Phenotypic values are calculated as normalized z-scores. (B)  
346 Principal component analysis (PCA) using the maximum specific growth rates under six  
347 microculture growth conditions, together with the distribution of hybrid strains. Arrows  
348 depict the different environmental conditions. (C) Best-parent heterosis in the 31 interspecific  
349 hybrids evaluated under microculture conditions in triplicates. (D) Fermentation capacity for  
350 the 31 interspecific hybrids and parental strains at 12 °C. Plotted values correspond to mean  
351 values of three independent replicates for each hybrid. Asterisk indicates different levels of  
352 significance compared to the commercial strain W34/70 (Student t-test; \*\*\*  $p \leq 0.001$  and  
353 \*\*\*\*  $p \leq 0.0001$ ). (E) Best-parent heterosis in the 31 interspecific hybrids evaluated under  
354 fermentation conditions at 12 °C.

355 To assess the impact of hybridization on yeast fitness, we calculated best-parent and mid-  
356 parent heterosis coefficients across the 31 hybrids (**Figure 1C, Table S3C-3D**). While some  
357 hybrids exhibited positive mid-parent heterosis in 5 out of 7 conditions (**Table S3C**), we  
358 generally did not observe hybrids with positive best-parent heterosis (BPH, **Table S3D**),  
359 except for rare cases involving maltose utilization and growth rate during diauxic shift, where  
360 2 and 5 hybrids, respectively, displayed positive values (**Figure 1C**). For example, in the  
361 H3.20-1 hybrid (L3 x CL710.1, generated at 20°C) we obtained a 74.8% BPH value for  
362 growth rate during diauxic shift. Overall, inter-species hybridization did not result in a  
363 significant enhancement of fitness in F1 hybrids.

364 Considering the potential use of these new hybrids for the production of Lager beer, we  
365 proceeded to assess the fermentation capacity of the 31 hybrids in wort at low temperature  
366 (**Figure 1D, Table S4**). Hybrids generated at 12 °C displayed similar levels of CO<sub>2</sub>  
367 production compared to those obtained at 20 °C (**Figure 1D, Table S4A**,  $p$ -value = 0.17,  
368 one-way ANOVA). We did not observe any hybrids exhibiting superior fermentative  
369 capacity when compared to their respective parental strains (**Figure S3**), and there was no  
370 evidence for hybrid vigour according to best-parent and mid-parent heterosis coefficients

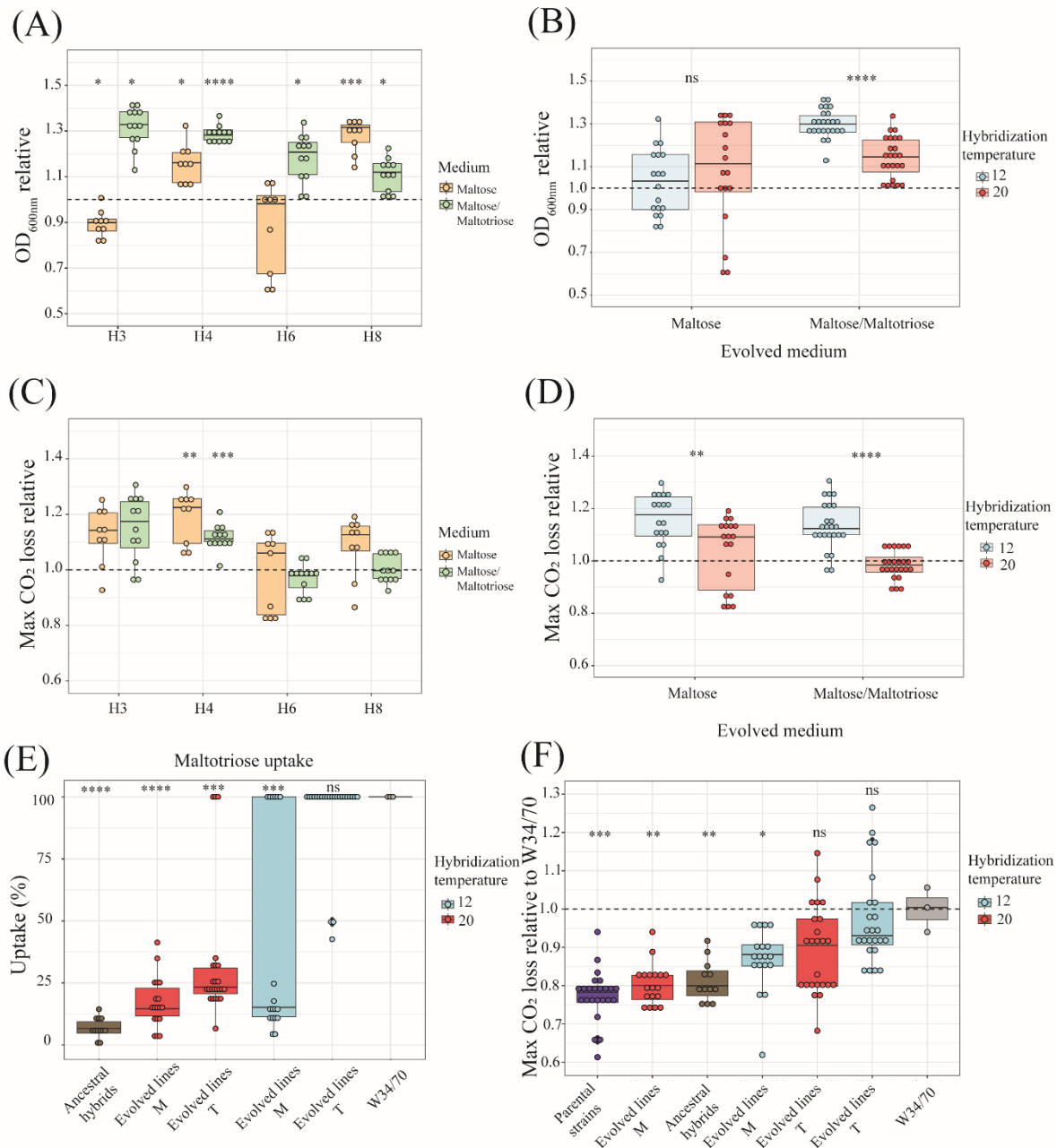
371 (Figure 1E, Table S4C-D). Neither parents nor hybrids reached the fermentative capacity  
372 of the commercial strain W34/70 (p-value < 0.05, one-way ANOVA).

373 **Evolved lines carrying the *S. eubayanus* mitochondria exhibit a greater fitness under**  
374 **fermentation.**

375 All results so far indicated that the *de novo* interspecific hybrids did not show any hybrid  
376 vigour, in none of the phenotypes assessed. We thus decided to subject hybrids to  
377 experimental evolution to enhance their fermentative capacity. We specifically selected four  
378 hybrids (H3.12-3, H4.12-4, H6.20-2, and H8.20-5) because they demonstrated the highest  
379 phenotypic values across kinetic parameters. From here on we will refer to these strains as  
380 H3-A, H4-A, H6-A and H8-A (A for ‘ancestral’ or unevolved hybrid). These four hybrids  
381 completely consumed the sugars present in the beer wort, except for maltotriose, which may  
382 explain the lower fermentative capacity of the hybrids compared to the commercial strain  
383 W34/70 (Table S4E). Furthermore, these four hybrids represent crosses made at 12 °C and  
384 20 °C and they encompass all six parental genetic backgrounds. To enhance the fermentative  
385 capacity of these selected hybrids, they were subjected to adaptive evolution at 20 °C for 250  
386 generations under two distinct conditions: i) YNB supplemented with 2% maltose and 9%  
387 ethanol (referred to as "M" medium), and ii) YNB supplemented with 1% maltose, 1%  
388 maltotriose, and 9% ethanol (referred to as "T" medium). We evolved three lines  
389 independently per cross in medium M, and four independent lines per cross in medium T.  
390 These conditions were chosen because maltose is the main sugar in beer wort (approximately  
391 60%) (Nikulin et al., 2018). Considering that yeast typically consume carbon sources in a  
392 specific order (glucose, fructose, maltose, and maltotriose), we employed a combination of  
393 maltose and maltotriose to facilitate the utilization of the latter carbon source.

394 After 250 generations, the evolved lines showed different levels of fitness improvements,  
395 depending on the environmental conditions and their genetic background (**Figure 2A, Figure**  
396 **S4**), with distinct fitness trajectories over time (**Figure S5**). All evolved lines significantly  
397 increased in fitness in at least one of the evolution media and/or kinetic parameters assessed  
398 compared to their respective ancestral hybrids (**Figure 2A, Table S5A-B**; p-value < 0.05,  
399 one-way ANOVA). Interestingly, evolved lines from hybrids made at 12 °C mating  
400 temperature (H3-A and H4-A) showed a more pronounced fitness increase in the T medium  
401 compared to those generated at 20 °C (p-value = 3.327e-08, one-way ANOVA, **Figure 2B**  
402 **and S4B**), suggesting that hybrids with *S. eubayanus* mitochondria have greater potential for  
403 improvement than hybrids with *S. cerevisiae* mitochondria. We verified that the two ancestral  
404 H3-A and H4-A hybrids carried only *S. eubayanus* mitochondria by sequencing the *COX3*  
405 gene, while H6-A and H8-A inherited the mitochondria from *S. cerevisiae* (**Table S5C-D**).

406



407

408 **Figure 2. Fitness of evolved lines under microcultures and fermentation conditions.** (A)  
 409 Mean relative fitness (maximum OD<sub>600nm</sub>) of evolved lines after 250 generations under  
 410 microculture conditions. Evolved lines were evaluated in the same medium where they were  
 411 evolved (M or T medium). (B) Comparison of mean relative fitness (maximum OD<sub>600nm</sub>)  
 412 shown in (A) between evolved lines from hybrids generated at 12 °C vs 20 °C. (C) Mean  
 413 relative fitness (maximum CO<sub>2</sub> loss) of evolved lines after 250 generation under fermentation  
 414 conditions at 12 °C. (D) Comparison of mean relative fitness (maximum CO<sub>2</sub> loss) shown in

415 (C) between evolved lines from hybrids generated at 12 °C vs 20 °C. (E) Maltotriose uptake  
416 of evolved hybrid lines in maltose (M) and maltose/maltotriose (T), relative to the  
417 commercial Lager strain W34/70. Ancestral hybrids are shown in grey, cold-generated and  
418 warm-generated hybrid lines are shown in blue and red, respectively. (F) Fermentative  
419 capacity of evolved individuals relative to the commercial Lager strain W34/70 grouped  
420 according to the environmental condition used during experimental evolution and  
421 hybridization temperature to generate the ancestral hybrid. Plotted values correspond to the  
422 mean of three independent biological replicates of each evolved line or strain. Asterisk  
423 represents different levels of significance (Students t-test, \*  $p \leq 0.05$ , \*\*  $p \leq 0.01$ , \*\*\*  $p \leq$   
424  $0.001$ , \*\*\*\*  $p \leq 0.0001$ , ns not significant).

425 Next, we assessed the fermentative capacity of the evolved lines under conditions resembling  
426 beer wort fermentation (12 °Brix and 12 °C) (**Figure 2C**, **Figure S6**, and **Table S6A-S6B**).

427 We did not observe a significant increase in CO<sub>2</sub> production levels in the evolved lines of the  
428 H6-A and H8-A hybrids in either M or T media (**Figure 2C**, **Figure S6** and **Table S6B**, p-  
429 value < 0.05, one-way ANOVA). However, we found a significant greater CO<sub>2</sub> production  
430 in the evolved lines of H4-A, evident in both evolution media, indicative of higher  
431 fermentation activity. The evolved lines of H3-A under T media also demonstrated a slightly  
432 higher CO<sub>2</sub> production (**Figure 2C** and **Table S6B**, p-value < 0.05, one-way ANOVA, for  
433 H4 evolved lines and p-values of 0.0708 and 0.05149 for H3 evolved lines in M and T,  
434 respectively). Thus, both evolved hybrids lines generated at cold-temperature, carrying *S.*  
435 *eubayanus* mitochondria, showed a greater increase in CO<sub>2</sub> production than hybrids carrying  
436 the *S. cerevisiae* mitochondria (**Figure 2C**). Specifically, hybrids with *S. eubayanus*  
437 mitochondria increased their maximum CO<sub>2</sub> loss by 10.6% when evolving in M medium (p-  
438 value = 0.003698, one-way ANOVA) and by 13% in T medium (p-value = 1.328e-08, one-  
439 way ANOVA) (**Figure 2D**). This was predominantly due to an elevated maltotriose uptake  
440 (**Figure 2E** and **Table S6C**). Notably, the fermentative capacity of these hybrids reached that  
441 of the commercial strain (**Table S6D**, p-value > 0.05, one-way ANOVA). These findings  
442 strongly suggest that lines derived from hybrids generated at colder temperatures carrying *S.*

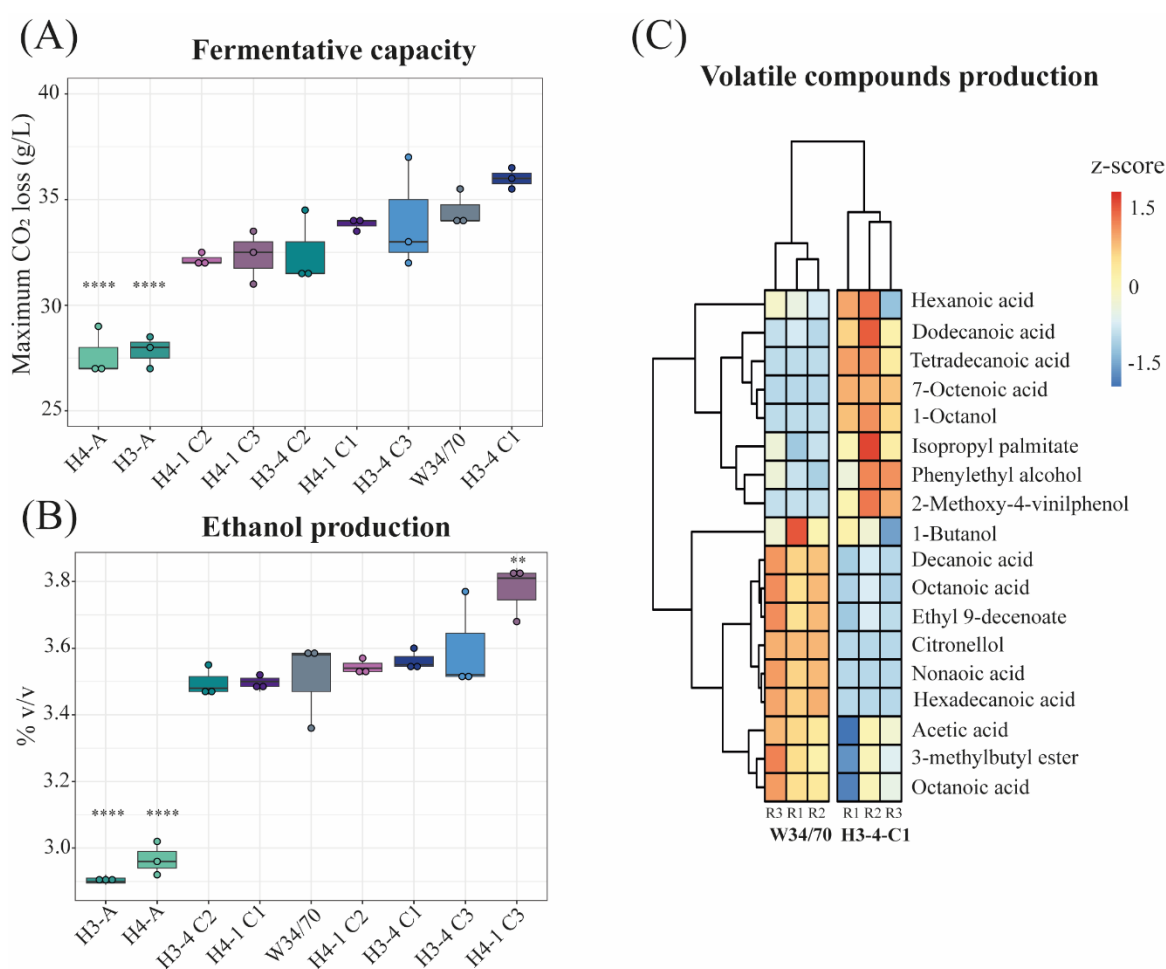
443 *eubayanus* mitochondria and evolved in a complex maltose/maltotriose medium (T),  
444 significantly enhanced their lager fermentative capacity due to an increase maltotriose uptake  
445 during beer wort fermentation.

#### 446 **Isolation of evolved genotypes with improved fermentative capacity and maltotriose** 447 **uptake**

448 To isolate individual representatives from the evolved population lines, we obtained one  
449 single genotype from each of the four hybrid lines at 250 generations (28 genotypes in total),  
450 which were then subjected to phenotypic evaluation in beer wort. These individual genotypes  
451 showed similar fermentation profiles as the population-level analyses above (**Figure 2F**).  
452 Evolved hybrid genotypes carrying *S. eubayanus* mitochondria and evolved in T medium  
453 (maltose/maltotriose, H3-E and H4-E), showed higher CO<sub>2</sub> production compared to H6-E  
454 and H8-E (p-value < 0.05, ANOVA, **Figure S7**). The genotypes with the largest significant  
455 fitness increase were derived from line H3-3 and H3-4 evolved in T conditions (**Figure S7**),  
456 which exceeded the commercial strain. Interestingly, two genotypes deriving from H6-A  
457 (carrying the *S. cerevisiae* mitochondria) evolved in T medium also showed a CO<sub>2</sub> loss  
458 similar to the commercial strain (p-value = 0.90372, one-way ANOVA).

459 To focus more in-depth on the evolved lines with the highest fermentative capacity and  
460 carrying the *S. eubayanus* mitochondria (H3-4 and H4-1 evolved in T medium, **Figure S7**),  
461 we isolated three colonies from each of these two lines to evaluate their fermentative  
462 capabilities. Notably, the CO<sub>2</sub> loss kinetics among these genotypes were comparable (p-value  
463 > 0.05, one-way ANOVA), with genotype #1 from line H3-4 exhibiting the highest CO<sub>2</sub> loss  
464 (**Figure 3A**). All these genotypes' fermentation profiles closely resembled that of the W34/70  
465 commercial Lager strain, underscoring the significantly high fermentative capacity of these

466 novel hybrids (p-value > 0.05, one-way ANOVA, **Figure 3A**). All genotypes consumed the  
 467 maltotriose in the T medium completely (**Table S7A**), and ethanol production ranged from  
 468 3.50% to 3.78% v/v (**Figure 3B**), which is similar to the commercial strain (p-value > 0.05,  
 469 one-way ANOVA). One genotype (H4-1-C3) showed a remarkable 7.1% increase in ethanol  
 470 production compared to the commercial strain (**Figure 3B**, p-value = 0.001, one-way  
 471 ANOVA).



472

473 **Figure 3. Fermentation performance of evolved hybrid individuals.** (A) Maximum CO<sub>2</sub>  
 474 loss (g/L) for three different isolated genotypes (C1-C3) from evolved lines H3-4 and H4-1,  
 475 ancestral hybrids (H3-A and H4-A) and commercial lager strain (W34/70). (B) Ethanol  
 476 production (% v/v) for strains evaluated in (A). (C) Hierarchically clustered heatmap of  
 477 volatile compounds production for strains evaluated in (A). Phenotypic values are calculated  
 478 as normalized z-scores. For (A) and (B), plotted values correspond to the mean of three



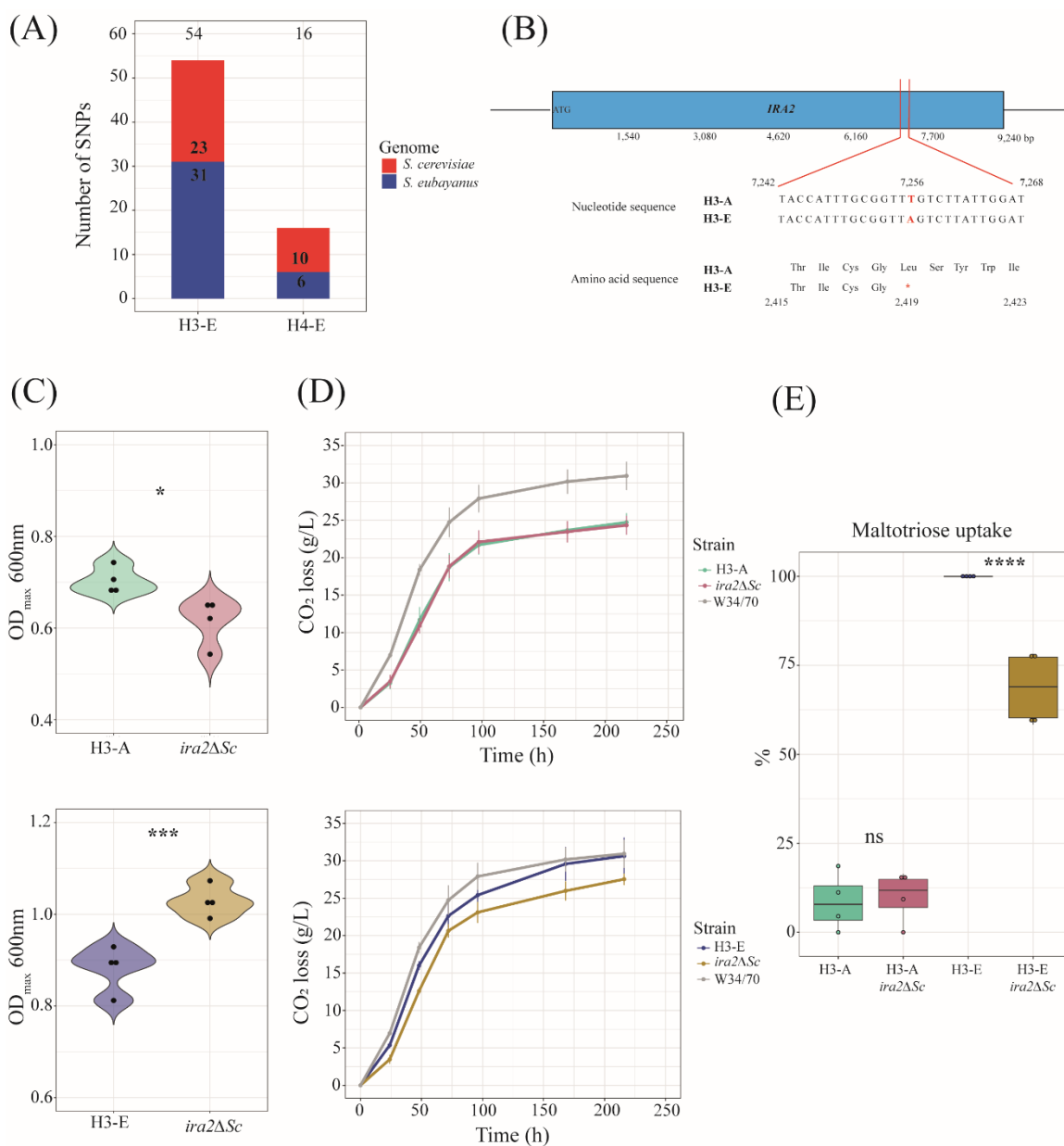
479 independent replicates. The (\*) represents different levels of significance between hybrids  
480 and commercial lager strain (Student t-test, \*\*  $p < 0.01$ , \*\*\*\*  $p < 0.0001$ ).

481 To compare the aroma profile of the H3-4-C1 evolved hybrid to the lager strain, we identified  
482 volatile compounds (VCs) by HS-SPME-GC-MS in the fermented wort. This assay allowed  
483 us to identify 15 and 14 compounds in the evolved and commercial lager strains, respectively.  
484 We observed significant differences for 11 different compounds (**Figure 3C**,  $p$ -value  $< 0.05$ ,  
485 one-way ANOVA, **Table S7B**), including ethyl esters and higher alcohols. For example, the  
486 evolved strain produced significantly more fatty acid ethyl ester, such as dodecanoic and  
487 tetradecanoic acid ethyl esters ( $p$ -value = 0.013 and 0.002, respectively, one-way ANOVA).  
488 The commercial lager strain on the other hand produced higher amounts of other ethyl esters,  
489 such as octanoic acid and nonanoic acid (**Figure 3D**,  $p$ -value = 0.001 and 0.0001,  
490 respectively, one-way ANOVA). The H3-4-C1 evolved hybrid produced detectable levels of  
491 4-vinyl guaiacol, which was completely absent in the lager strain. These results demonstrate  
492 that the aroma profiles of the evolved hybrids differ from the commercial lager strain.

### 493 **Evolved hybrids have mutations in genes related to carbon metabolism**

494 To identify mutations in evolved hybrids associated with their improved fermentative  
495 capacity, we sequenced the genomes of the two genotypes exhibiting the highest CO<sub>2</sub>  
496 production levels, specifically H3-4-C1 and H4-1-C1 (from here on referred to as H3-E and  
497 H4-E; with 'E' for evolved hybrid) that were evolved in the maltose/maltotriose T medium  
498 (**Table S8A**). Genome sequencing revealed that these two backgrounds had equal  
499 contributions from both parental genomes, that they had euploid, diploid genomes with no  
500 detectable aneuploidies (**Table S8B**), and that they contained *S. eubayanus* mitochondria.

501 We then identified *de novo* single nucleotide polymorphisms (SNPs) in the evolved hybrid  
502 genomes that were absent in the ancestral hybrids. We found 54 and 16 SNPs in the H3-E  
503 and H4-E backgrounds, respectively (**Table S8C**). The evolved hybrids differed in the total  
504 number of SNPs per genome (**Figure 4A**). In H3-E, we found 23 and 31 SNPs in the *S.*  
505 *cerevisiae* and *S. eubayanus* parental genomes, respectively, while H4-E only had 10 and 6  
506 SNPs in the corresponding parental genomes. A GO-term analysis identified that many  
507 mutations in H3-E impacted genes related to ‘maltose metabolic process’, while in H4-E  
508 mostly ‘fungal-type cell wall organization’ genes were hit (**Figure S8**). We detected 27 SNPs  
509 within coding genes, of which six were related to maltose metabolism in the H3-E hybrid  
510 (**Table S8C**). For example, we identified an anticipated stop-codon in the *IRA2* allele  
511 (encoding for a GTPase-activating protein, **Figure 4B**) in the *S. cerevisiae* sub-genome, and  
512 a missense mutation in *MAL32* (encoding for a maltase enzyme) and *SNF3* (encoding for a  
513 plasma membrane low glucose sensor) in the *S. eubayanus* sub-genome (**Table S8C**), which  
514 are all genes related to sugar consumption.



515

516 **Figure 4. Genomic analysis of evolved hybrids.** (A) Total number of *de novo* SNPs in the  
517 H3-E and H4-E hybrids. (B) SNP present in the *IRA2* gene in the *S. cerevisiae* sub-genome  
518 in the H3-E hybrid. (C) Maximum OD<sub>600nm</sub> of *ira2ΔSc* mutant strains under microculture  
519 conditions. Mutant and wild-type strains were evaluated in the T medium. (D) CO<sub>2</sub> loss  
520 kinetics for *ira2ΔSc* mutant and wild-type strains. (E) Maltotriose uptake (%) for strains  
521 evaluated in (D). For (C), (D) and (E), plotted values correspond to the mean of four  
522 independent replicates. The (\*) represents different levels of significance between mutant  
523 and wild-type strains (Student t-test, \* p < 0.05, \*\*\* p < 0.001, \*\*\*\* p < 0.0001).

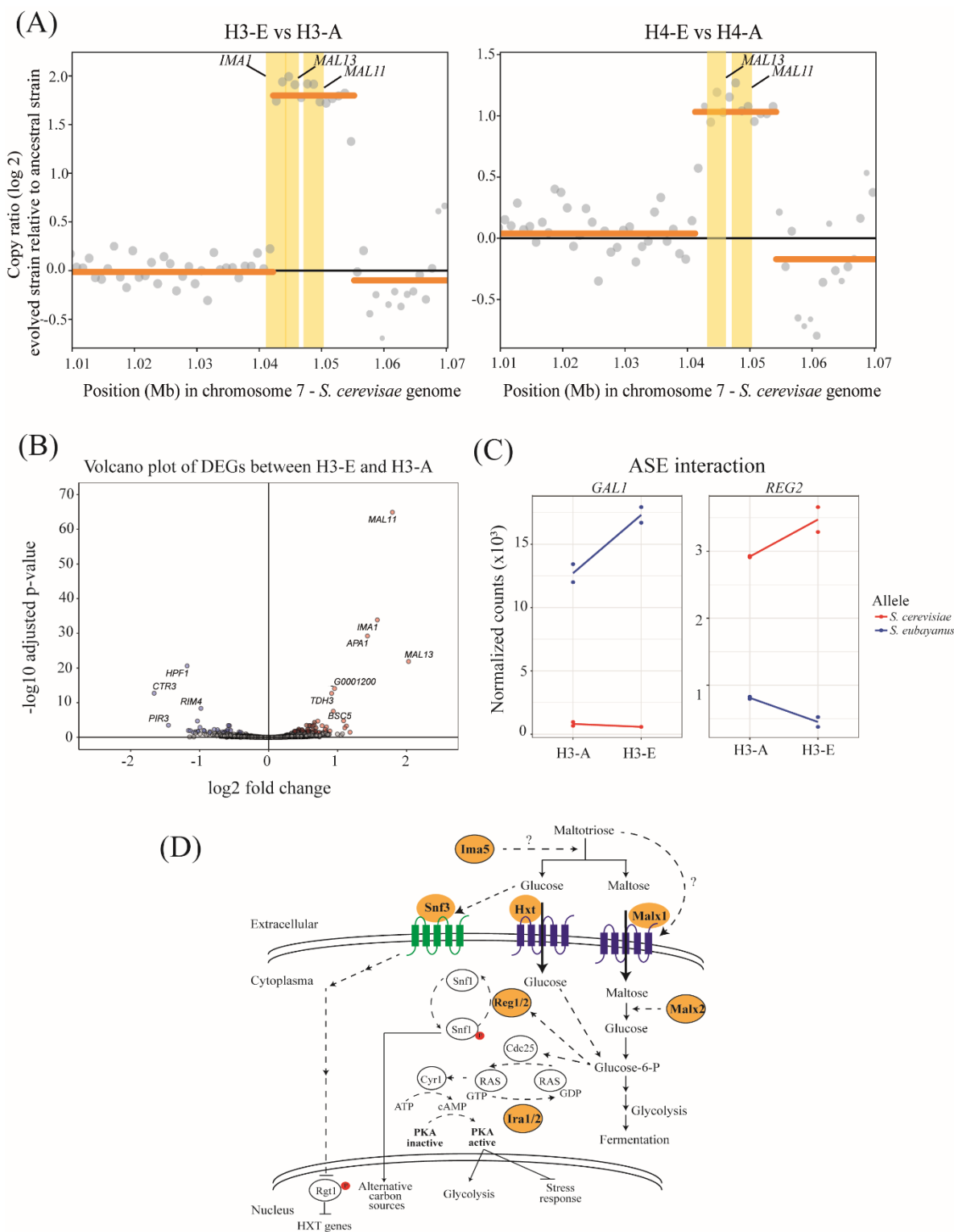
524 To track the relative frequencies of the *IRA2*, *MAL32* and *SNF3* polymorphisms in the H3  
525 evolution line, we sequenced whole population samples at increasing timepoints of  
526 experimental evolution (at 50, 100, 150, 200, and 250 generations; **Figure S9**). The *IRA2*-  
527 L2418\* polymorphism arose before generation 50 and was completely fixed by 150  
528 generations. Conversely, *MAL32* (K99N and L100Q) and *SNF3* (A493T) mutations only  
529 occurred late in evolution, between 200 and 250 generations, at low frequencies (10%).

530 To determine the phenotypic impact of the stop-codon detected in the *IRA2* gene, we  
531 performed a CRISPR assay targeting the *S. cerevisiae IRA2*, generating null mutants (*ira2<sup>Sc</sup>*)  
532 in the evolved and non-evolved hybrids. We evaluated growth under microculture conditions  
533 in the same evolutionary medium (T) and under beer wort fermentation (**Figure 4C**). This  
534 assay revealed that *ira2<sup>Sc</sup>* mutants in the H3-A hybrid background had a 12.5% lower OD<sub>max</sub>  
535 under maltose/maltotriose conditions compared to H3-A (**Figure 4C**, p-value = 0.01213,  
536 one-way ANOVA), but still a similar fermentative capacity (**Figure 4D**, p-value = 0.79685,  
537 one-way ANOVA). In the H3-E hybrid, the null *ira2<sup>Sc</sup>* mutant showed a 16.6% higher OD<sub>max</sub>  
538 under microculture conditions (**Figure 4C**, p-value = 0.00042, one-way ANOVA) and a  
539 significantly lower fermentative capacity under beer wort, with a 13.6% decrease in CO<sub>2</sub>  
540 production (**Figure 4D**, p-value = 0.02315 one-way ANOVA, **Table S9**) and a 10.8%  
541 decrease in the maximum CO<sub>2</sub> loss rate (**Table S9**, p-value = 0.02268 one-way ANOVA).  
542 This decrease in the fermentative capacity in the H3-E null mutant correlates with a lower  
543 maltotriose uptake (68.6%, **Figure 4E**). These results suggest that the stop-codon in *IRA2* in  
544 the evolved hybrids does not necessarily lead to a loss of protein function, but instead to a  
545 complex genetic interaction in the H3-E background promoting a trade-off between biomass

546 and fermentative capacity, which is likely partly responsible for the phenotypic differences  
547 during the evolutionary process.

548 **Copy number variants of genes related to maltose metabolism are associated with**  
549 **improved fermentative capacity in evolved hybrids.**

550 Since *ira2* null mutants did not restore the full increase in fermentative capacity of the  
551 evolved hybrids, we examined genes exhibiting copy number variation (CNVs) in H3-E and  
552 H4-E hybrids (**Figure 5A, Table S8D**). Both H3-E and H4-E hybrids contained changes in  
553 copy number, particularly in the *MAL* gene family (**Figure 5A, Table S8D**). For example,  
554 we identified 2 and 4 extra copies of the *MAL13* and *MAL11* genes in H4-E and H3-E,  
555 respectively.



556

557 **Figure 5. Copy number variation and differential gene expression analysis.** (A) Copy  
 558 number variations (CNVs) between H3-E and H4-E hybrids relative to their ancestral hybrids  
 559 found in *S. cerevisiae* chromosome 7. Coding genes located within bins showing CNV calls

560 higher than 1 copy (yellow rectangles) are shown. **(B)** Volcano plot showing differential  
561 expressed genes (DEGs) between H3-E and H3-A hybrids. The red and blue dots represent  
562 up-regulated and down-regulated genes in the H3-E hybrids, respectively. **(C)** Orthologous  
563 genes showing an interaction between allelic expression and experimental evolution. **(D)**  
564 Model depicting genes exhibiting mutations after the experimental evolution assay  
565 (highlighted in orange) and involved in pathways related to the detection, regulation, uptake,  
566 and catabolism of maltotriose. Phosphorylation is indicated in red. Green depicts a glucose  
567 sensing protein, while proteins in blue highlight transporters involved in sugar consumption.

568 To determine the impact of these mutations and the CNVs in the transcriptome of the H3-E  
569 hybrid, we estimated transcript abundance under beer fermentative conditions in the evolved  
570 and non-evolved hybrid. We identified 40 Differentially Expressed Genes (DEGs, FDR <  
571 5%, **Table S8E**), where 21 and 19 genes were up- and down regulated in the evolved hybrid  
572 relative to its hybrid ancestor, respectively. Interestingly, we found that *S. cerevisiae* alleles  
573 for *IMAI*, *MAL11*, and *MAL13* were up-regulated in H3-E, which correlates with the  
574 increased gene copy number (**Figure 5B**). A GO term analysis showed that genes involved  
575 in maltose metabolic processes were up-regulated and genes in cell wall organization were  
576 down-regulated in the evolved hybrid, which correlates with the genetic changes we  
577 identified in coding regions (**Table S8F**).

578 To measure the impact of *cis*-variants on allelic expression within each parental subgenome,  
579 we estimated allele specific expression (ASE) in the evolved and non-evolved hybrids  
580 (**Figure 5C, Table S8G**). Seven genes showed ASE differences between the evolved and  
581 ancestral hybrid, likely originating from mutations in regulatory regions acquired during  
582 experimental evolution (**Figure 5C, Table S8G**). Of these, one and six ASE differences in  
583 the H3-E hybrid represented up-regulated alleles in the *S. cerevisiae* and *S. eubayanus*  
584 subgenomes, respectively (**Table S8G**). Interestingly, we detected the up-regulation of the  
585 *REG2* allele related to sugar consumption with a 2.1 higher fold change in the *S. cerevisiae*

586 subgenome, which is involved in regulation of glucose-repressible genes (**Figure 5C**),  
587 correlating with the higher maltose and maltotriose consumption levels in the evolved hybrid.

## 588 **DISCUSSION**

589 The hybrid yeast strains traditionally used for Lager beer production (*S. pastorianus*) are  
590 highly limited in genetic diversity. Currently, only two types of strains are used worldwide  
591 (Bonatto, 2021; Gallone et al., 2019; Gorter De Vries, Pronk, et al., 2019; Langdon et al.,  
592 2019), stemming from a single hybridization event that gave rise to the current Lager strains.  
593 This strongly constrains the diversity of available flavour and aroma profiles. The genetically  
594 depleted landscape of Lager strains also prevents a comprehensive understanding of the  
595 genetic changes crucial for the domestication process (Gallone et al., 2019; Langdon et al.,  
596 2019). The recent discovery of genetically and phenotypically distinct *S. eubayanus* lineages,  
597 including isolates from Patagonia (Eizaguirre et al., 2018; Langdon et al., 2020; Libkind et  
598 al., 2011; Nespolo et al., 2020), opened new avenues for understanding Lager yeast  
599 domestication, and to develop new strains to increase the diversity of fermentation profiles  
600 (Cubillos et al., 2019; Gibson et al., 2017). Previous studies using hybridization and  
601 experimental evolution demonstrated that Lager yeast hybrids could be improved through  
602 selection under fermentation conditions (Krogerus, Preiss, et al., 2018) without  
603 polyploidization (Krogerus et al., 2015). While these studies have expanded the diversity of  
604 Lager yeast phenotypes, they are primarily based on a single *S. eubayanus* genetic  
605 background, CBS 12357T (belonging to PB-1), which is not representative of the overall  
606 species' genetic and phenotypic diversity (Burini et al., 2021; Molinet, Eizaguirre, et al.,  
607 2022; Nespolo et al., 2020; Urbina et al., 2020). *S. eubayanus* lineages vary widely in  
608 fermentation capacity and aroma profiles during beer fermentation, suggesting that the



609 natural diversity of *S. eubayanus* is also well-suited for making innovative Lager hybrid  
610 strains (Burini et al., 2021; Mardones et al., 2021; Urbina et al., 2020). Here, we expanded  
611 the strain repertoire available for Lager brewing by including all three different *S. eubayanus*  
612 lineages found in Patagonia. Leveraging the genetic diversity of *S. eubayanus*, we created  
613 novel *S. cerevisiae* x *S. eubayanus* hybrids and enhanced their fermentation capacity through  
614 experimental evolution. We show that desirable phenotypic outcomes such as high ethanol  
615 production and new aroma profiles are the result of an intricate interplay of pre-existing  
616 genetic diversity, and selection on species-specific mitochondria, *de novo* mutations in sugar  
617 consumption genes, together with CNV of the *MAL* genes, important to improve maltose  
618 consumption during fermentation.

619 Hybridization offers a mechanism to combine beneficial traits from different species, which  
620 can enable adaptation to new environmental conditions (Gabaldón, 2020; R. Stelkens &  
621 Bendixsen, 2022) and improve the yield of plant cultivars and animal breeds (Adavoudi &  
622 Pilot, 2022; Rieseberg et al., 2003; Seehausen, 2004). However, hybridization - without  
623 subsequent selection of desirable traits for multiple generations - may not be sufficient to  
624 generate new phenotypes. None of the initial F1 hybrids in our experiment showed best  
625 parent heterosis, demonstrating that hybridization at different temperatures alone, was not  
626 sufficient to generate hybrids with a greater fitness than their parents under fermentative  
627 conditions. We therefore turned to experimental evolution as an alternative approach to  
628 improve the hybrids' fermentative profiles. Experimental evolution across multiple  
629 generations, paired with time-series whole genome sequencing, is a powerful tool for  
630 studying microbial responses to a selective environment and to understand the fitness effects  
631 of *de novo* mutations (Barrick & Lenski, 2013; Burke, 2023; Cooper, 2018; Maddamsetti et

632 al., 2015). We found that, after 250 generations in a high sugar and ethanol environment,  
633 hybrids evolved faster fermentation performance and higher ethanol production compared to  
634 both parents and ancestral unevolved hybrids. Interestingly, the hybrids' evolutionary  
635 potential relied on the parental mitochondria. Hybrids with *S. eubayanus* mitochondria  
636 demonstrated higher fitness post-experimental evolution than those with *S. cerevisiae*  
637 mitochondria. Consistent with our results, all Lager commercial hybrids have *S. eubayanus*  
638 mitochondria (Gallone et al., 2019; Gorter De Vries, Pronk, et al., 2019; Langdon et al.,  
639 2019). It has been demonstrated that in synthetic hybrids, *S. eubayanus* mitochondria confers  
640 vigorous growth at colder temperatures compared to the *S. cerevisiae* mitotype, potentially  
641 conferring a competitive advantage in the cooler brewing conditions typical of Lagers (Baker  
642 et al., 2019). However, we performed experimental evolution at warmer temperatures (25°C).  
643 It is thus plausible that species-specific mitochondrial effects play an additional role,  
644 specifically concerning sugar utilization and glucose repression (Ulery et al., 1994), when  
645 adapting to Lager brewing conditions. These mitochondrial effects likely involve complex  
646 genetic interactions with the nuclear genome and might be exacerbated in the presence of the  
647 *S. eubayanus* mitochondria.

648 Our genome-wide screens for mutations to elucidate the genetic basis of hybrid fitness  
649 improvement identified several *de novo* SNPs and CNVs in the genomes of the evolved  
650 hybrids. These genetic changes were identified in genes with known effects on maltose  
651 metabolism and cell wall organization (**Figure 5D**). Particularly interesting are mutations in  
652 *IRA2* in the *S. cerevisiae* subgenome and in *SNF3* in the *S. eubayanus* sub-genome, which  
653 are both related to carbon metabolism. Evolved hybrids carried a premature stop codon in  
654 the *IRA2* gene, which was absent in both the *S. cerevisiae* and *S. eubayanus* parental

655 ancestors, and in the unevolved hybrids at the beginning of experimental evolution. *SNF3*  
656 encodes for a low-glucose sensor and regulates the expression of hexose transporters  
657 (Santangelo, 2006), where *snf3* yeast mutants have low fitness in environments with low  
658 glucose concentrations (Vagnoli & Bisson, 1998). *IRA2* is a known suppressor of *snf3*  
659 mutants (Ramakrishnan et al., 2007), with *IRA2* required for reducing cAMP levels under  
660 nutrient limited conditions, where cAMP directly regulates the activity of several key  
661 enzymes of glycolysis (François & Parrou, 2001; Ramakrishnan et al., 2007). A mutation in  
662 *IRA2* would increase the carbon flux through glycolysis, which is in agreement with our  
663 finding that evolved hybrids showed higher sugar consumption. Furthermore, the regulation  
664 of the yeast mitochondrial function in response to nutritional changes can be modulated by  
665 cAMP/PKA signalling (Leadsham & Gourlay, 2010), which might be exacerbated in strains  
666 carrying *S. eubayanus* mitochondria. We further consolidated this mechanism by CNV and  
667 transcriptome analyses, which detected several up-regulated genes related to maltose  
668 consumption in the evolved hybrid during fermentation. Furthermore, the newly generated  
669 hybrids exhibited a distinct volatile compound profile compared to the W34/70 Lager strain.  
670 This highlights the potential of wild Patagonian yeast to introduce diversity into the current  
671 repertoire of available Lager yeasts. Previous studies in laboratory-made Lager hybrids  
672 revealed genetic changes that significantly impacted fermentation performance and changed  
673 the aroma profile of the resulting beer, compared to the commercial Lager strain (Gibson et  
674 al., 2020; Krogerus, Preiss, et al., 2018).

675 In summary, our study expands the genetic diversity of Lager hybrids and shows that new *S.*  
676 *cerevisiae* x *S. eubayanus* hybrids can be generated from wild yeast strains isolated from  
677 Patagonia. We found that hybridization at low temperatures, selecting for the retention of *S.*

678 *eubayanus* mitochondria, followed by experimental evolution under fermentative conditions,  
679 and selection on desirable traits (ethanol production and aroma profiles), can generate hybrid  
680 strains with enhanced fermentation capacities. We delineate how genetic changes within  
681 distinct subgenomes of the hybrids contribute to improved fermentation efficacy, specifically  
682 in the context of cold Lager brewing conditions. This opens up new opportunities for the  
683 brewing industry to alleviate current constraints in Lager beer production, and to expand the  
684 range of currently available Lager beer styles.

## 685 **ACKNOWLEDGMENTS**

686 We thank Antonio Molina, José Ruiz, Kamila Urbina, Mirjam Amcoff, Elin Gülich and S.  
687 Lorena Ament-Velásquez for their technical help. We also acknowledge Fundación Ciencia  
688 & Vida for providing infrastructure, laboratory space and equipment for experiments. This  
689 research was partially supported by the supercomputing infrastructure of the National  
690 Laboratory for High Performance Computing Chile (NLHPC, ECM-02) and by SNIC  
691 through Uppsala Multidisciplinary Center for Advanced Computational Science (UPPMAX)  
692 under Project naiss2023-22-62.

## 693 **FUNDING**

694 This research was funded by Agencia Nacional de Investigación y Desarrollo (ANID)  
695 FONDECYT program and ANID-Programa Iniciativa Científica Milenio – ICN17\_022 and  
696 NCN2021\_050. FC is supported by FONDECYT grant N° 1220026, JM by FONDECYT  
697 POSTDOCTORADO grant N° 3200545 and PV by ANID FONDECYT  
698 POSTDOCTORADO grant N° 3200575. CV is supported by FONDECYT INICIACIÓN  
699 grant N° 11230724. RN is supported by FONDECYT grant N° 1221073. RS and JM’s work

700 is supported by the Swedish Research Council (2022-03427) and the Knut and Alice  
701 Wallenberg Foundation (2017.0163).

## 702 **AUTHOR CONTRIBUTIONS**

703 Conceptualization: J.M., F.A.C.; Investigation: J.M., C.A.V., F.A.C.; Methodology: J.M.,  
704 J.P.N., F.I.S., F.A.C.; Software: J.M., C.A.V., P.V.; Formal Analysis: J.M., J.P.N., R.S.,  
705 F.A.C.; Resources: J.M., P.V., R.S., R.F.N., F.A.C.; Visualization: J.M., J.P.N., C.A.V.,  
706 P.V.; Original Draft Preparation: J.M., C.A.V., R.S., F.A.C. All authors have read and agreed  
707 to the published version of the manuscript.

## 708 **Competing interests**

709 The authors declare no conflict of interest.

## 710 **REFERENCES**

- 711 Abbott, R., Albach, D., Ansell, S., Arntzen, J. W., Baird, S. J. E., Bierne, N., Boughman, J.,  
712 Brelsford, A., Buerkle, C. A., Buggs, R., Butlin, R. K., Dieckmann, U., Eroukhmanoff,  
713 F., Grill, A., Cahan, S. H., Hermansen, J. S., Hewitt, G., Hudson, A. G., Jiggins, C., ...  
714 Zinner, D. (2013). Hybridization and speciation. *Journal of Evolutionary Biology*,  
715 26(2), 229–246. <https://doi.org/10.1111/j.1420-9101.2012.02599.x>
- 716 Adavoudi, R., & Pilot, M. (2022). Consequences of hybridization in mammals: A systematic  
717 review. *Genes*, 13(1). <https://doi.org/10.3390/genes13010050>
- 718 Alexa, A., & Rahnenfuhrer, J. (2023). *topGO: Enrichment Analysis for Gene Ontology.R*  
719 *package version 2.54.0*. <https://doi.org/10.18129/B9.bioc.topGO>
- 720 Baker, E. C. P., Peris, D., Moriarty, R. V., Li, X. C., Fay, J. C., & Hittinger, C. T. (2019).  
721 Mitochondrial DNA and temperature tolerance in lager yeasts. *Science Advances*, 5(1),  
722 1–8. <https://doi.org/10.1126/sciadv.aav1869>

- 723 Barrick, J. E., & Lenski, R. E. (2013). Genome dynamics during experimental evolution.  
724 *Nature Reviews Genetics*, *14*(12), 827–839. <https://doi.org/10.1038/nrg3564>
- 725 Bernardes, J. P., Stelkens, R. B., & Greig, D. (2017). Heterosis in hybrids within and between  
726 yeast species. *Journal of Evolutionary Biology*, *30*(3), 538–548.  
727 <https://doi.org/10.1111/jeb.13023>
- 728 Bonatto, D. (2021). The diversity of commercially available ale and lager yeast strains and  
729 the impact of brewer’s preferential yeast choice on the fermentative beer profiles. *Food*  
730 *Research International*, *141*(January), 110125.  
731 <https://doi.org/10.1016/j.foodres.2021.110125>
- 732 Brouwers, N., Brickwedde, A., Gorter de Vries, A., van den Broek, M., Weening, S., van den  
733 Eijnden, L., Diderich, J., Bai, F.-Y., Pronk, J., & Daran, J.-M. (2019). Maltotriose  
734 consumption by hybrid *Saccharomyces pastorianus* is heterotic and results from  
735 regulatory cross-talk between parental sub-genomes. *BioRxiv*, 679563.  
736 <https://doi.org/10.1101/679563>
- 737 Burini, J. A., Eizaguirre, J. I., Loviso, C., & Libkind, D. (2021). Non-conventional yeasts as  
738 tools for innovation and differentiation in brewing. *Revista Argentina de Microbiologia*,  
739 *53*(4). <https://doi.org/10.1016/j.ram.2021.01.003>
- 740 Burke, M. K. (2023). Embracing Complexity: Yeast Evolution Experiments Featuring  
741 Standing Genetic Variation. *Journal of Molecular Evolution*, *91*(3), 281–292.  
742 <https://doi.org/10.1007/s00239-023-10094-4>
- 743 Chen, S., Zhou, Y., Chen, Y., & Gu, J. (2018). Fastp: An ultra-fast all-in-one FASTQ  
744 preprocessor. *Bioinformatics*, *34*(17), i884–i890.  
745 <https://doi.org/10.1093/bioinformatics/bty560>
- 746 Cingolani, P., Platts, A., Wang, L. L., Coon, M., Nguyen, T., Wang, L., Land, S. J., Lu, X.,  
747 & Ruden, D. M. (2012). A program for annotating and predicting the effects of single  
748 nucleotide polymorphisms, SnpEff. *Fly*, *6*(2), 80–92. <https://doi.org/10.4161/fly.19695>
- 749 Cooper, V. S. (2018). Experimental Evolution as a High-Throughput Screen for Genetic

- 750 Adaptations. *MSphere*, 3(3), 1–7. <https://doi.org/10.1128/msphere.00121-18>
- 751 Cubillos, F. A., Gibson, B., Grijalva-Vallejos, N., Krogerus, K., & Nikulin, J. (2019).  
752 Bioprospecting for brewers: Exploiting natural diversity for naturally diverse beers.  
753 *Yeast*. <https://doi.org/10.1002/yea.3380>
- 754 Danecek, P., Auton, A., Abecasis, G., Albers, C. A., Banks, E., DePristo, M. A., Handsaker,  
755 R. E., Lunter, G., Marth, G. T., Sherry, S. T., McVean, G., & Durbin, R. (2011). The  
756 variant call format and VCFtools. *Bioinformatics*, 27(15), 2156–2158.  
757 <https://doi.org/10.1093/bioinformatics/btr330>
- 758 Danecek, P., Bonfield, J. K., Liddle, J., Marshall, J., Ohan, V., Pollard, M. O., Whitwham,  
759 A., Keane, T., McCarthy, S. A., & Davies, R. M. (2021). Twelve years of SAMtools  
760 and BCFtools. *GigaScience*, 10(2), 1–4. <https://doi.org/10.1093/gigascience/giab008>
- 761 Depristo, M. A., Banks, E., Poplin, R., Garimella, K. V., Maguire, J. R., Hartl, C.,  
762 Philippakis, A. A., Del Angel, G., Rivas, M. A., Hanna, M., McKenna, A., Fennell, T.  
763 J., Kernysky, A. M., Sivachenko, A. Y., Cibulskis, K., Gabriel, S. B., Altshuler, D., &  
764 Daly, M. J. (2011). A framework for variation discovery and genotyping using next-  
765 generation DNA sequencing data. *Nature Genetics*, 43(5), 491–501.  
766 <https://doi.org/10.1038/ng.806>
- 767 Dicarlo, J. E., Norville, J. E., Mali, P., Rios, X., Aach, J., & Church, G. M. (2013). Genome  
768 engineering in *Saccharomyces cerevisiae* using CRISPR-Cas systems. *Nucleic Acids*  
769 *Research*, 41(7), 4336–4343. <https://doi.org/10.1093/nar/gkt135>
- 770 Dobin, A., Davis, C. A., Schlesinger, F., Drenkow, J., Zaleski, C., Jha, S., Batut, P., Chaisson,  
771 M., & Gingeras, T. R. (2013). STAR: Ultrafast universal RNA-seq aligner.  
772 *Bioinformatics*, 29(1), 15–21. <https://doi.org/10.1093/bioinformatics/bts635>
- 773 Eizaguirre, J. I., Peris, D., Rodríguez, M. E., Lopes, C. A., De Los Ríos, P., Hittinger, C. T.,  
774 & Libkind, D. (2018). Phylogeography of the wild Lager-brewing ancestor  
775 (*Saccharomyces eubayanus*) in Patagonia. *Environmental Microbiology*, 20(10), 3732–  
776 3743. <https://doi.org/10.1111/1462-2920.14375>



- 777 Esteve-Zarzoso, B., Belloch, C., Uruburu, F., & Querol, A. (1999). Identification of yeasts  
778 by RFLP analysis of the 5.8S rRNA gene and the two ribosomal internal transcribed  
779 spacers. *International Journal of Systematic Bacteriology*, 49(1), 329–337.  
780 <https://doi.org/10.1099/00207713-49-1-329>
- 781 Fleiss, A., O'Donnell, S., Fournier, T., Lu, W., Agier, N., Delmas, S., Schacherer, J., &  
782 Fischer, G. (2019). Reshuffling yeast chromosomes with CRISPR/Cas9. *PLOS*  
783 *Genetics*, 15(8), e1008332. <https://doi.org/10.1371/journal.pgen.1008332>
- 784 François, J., & Parrou, J. L. (2001). Reserve carbohydrates metabolism in the yeast  
785 *Saccharomyces cerevisiae*. *FEMS Microbiology Reviews*, 25(1), 125–145.  
786 [https://doi.org/10.1016/S0168-6445\(00\)00059-0](https://doi.org/10.1016/S0168-6445(00)00059-0)
- 787 Gabaldón, T. (2020). Hybridization and the origin of new yeast lineages. *FEMS Yeast*  
788 *Research*, 20(5), 1–8. <https://doi.org/10.1093/femsyr/foaa040>
- 789 Gallone, B., Steensels, J., Mertens, S., Dzialo, M. C., Gordon, J. L., Wauters, R., Theßeling,  
790 F. A., Bellinazzo, F., Saels, V., Herrera-Malaver, B., Prahl, T., White, C., Hutzler, M.,  
791 Meußdoerffer, F., Malcorps, P., Souffriau, B., Daenen, L., Baele, G., Maere, S., &  
792 Verstrepen, K. J. (2019). Interspecific hybridization facilitates niche adaptation in beer  
793 yeast. *Nature Ecology and Evolution*, 3(11), 1562–1575.  
794 <https://doi.org/10.1038/s41559-019-0997-9>
- 795 Garrison, E., & Marth, G. (2012). Haplotype-based variant detection from short-read  
796 sequencing. *ArXiv*, 1–9. <http://arxiv.org/abs/1207.3907>
- 797 Gibson, B., Dahabieh, M., Krogerus, K., Jouhten, P., Magalhães, F., Pereira, R., Siewers, V.,  
798 & Vidgren, V. (2020). Adaptive Laboratory Evolution of Ale and Lager Yeasts for  
799 Improved Brewing Efficiency and Beer Quality. *Annual Review of Food Science and*  
800 *Technology*, 11(1). <https://doi.org/10.1146/annurev-food-032519-051715>
- 801 Gibson, B., Geertman, J. M. A., Hittinger, C. T., Krogerus, K., Libkind, D., Louis, E. J.,  
802 Magalhães, F., & Sampaio, J. P. (2017). New yeasts-new brews: Modern approaches to  
803 brewing yeast design and development. *FEMS Yeast Research*, 17(4), 1–13.



- 804 <https://doi.org/10.1093/femsyr/fox038>
- 805 Gorter De Vries, A. R., Pronk, J. T., & Daran, J. M. G. (2019). Lager-brewing yeasts in the  
806 era of modern genetics. *FEMS Yeast Research*, *19*(7), 1–17.  
807 <https://doi.org/10.1093/femsyr/foz063>
- 808 Gorter De Vries, A. R., Voskamp, M. A., Van Aalst, A. C. A., Kristensen, L. H., Jansen, L.,  
809 Van Den Broek, M., Salazar, A. N., Brouwers, N., Abeel, T., Pronk, J. T., & Daran, J.  
810 M. G. (2019). Laboratory evolution of a *Saccharomyces cerevisiae* × *S. eubayanus*  
811 hybrid under simulated lager-brewing conditions. *Frontiers in Genetics*, *10*(MAR).  
812 <https://doi.org/10.3389/fgene.2019.00242>
- 813 Hewitt, S. K., Duangrattanalert, K., Burgis, T., Zeef, L. A. H., Naseeb, S., & Delneri, D.  
814 (2020). Plasticity of Mitochondrial DNA Inheritance and its Impact on Nuclear Gene  
815 Transcription in Yeast Hybrids. *Microorganisms*, *8*(4), 494.  
816 <https://doi.org/10.3390/microorganisms8040494>
- 817 Horwitz, A. A., Walter, J. M., Schubert, M. G., Kung, S. H., Hawkins, K., Platt, D. M.,  
818 Hernday, A. D., Mahatdejkul-Meadows, T., Szeto, W., Chandran, S. S., & Newman, J.  
819 D. (2015). Efficient Multiplexed Integration of Synergistic Alleles and Metabolic  
820 Pathways in Yeasts via CRISPR-Cas. *Cell Systems*, *1*(1), 88–96.  
821 <https://doi.org/10.1016/j.cels.2015.02.001>
- 822 Hutzler, M., Morrissey, J. P., Laus, A., Meussdoerffer, F., & Zarnkow, M. (2023). A new  
823 hypothesis for the origin of the lager yeast *Saccharomyces pastorianus*. *FEMS Yeast*  
824 *Research*, *23*, 1–17. <https://doi.org/10.1093/femsyr/foad023>
- 825 Ibstedt, S., Stenberg, S., Bagés, S., Gjuvslund, A. B., Salinas, F., Kourtchenko, O., Samy, J.  
826 K. A., Blomberg, A., Omholt, S. W., Liti, G., Beltran, G., & Warringer, J. (2015).  
827 Concerted Evolution of Life Stage Performances Signals Recent Selection on Yeast  
828 Nitrogen Use. *Molecular Biology and Evolution*, *32*(1), 153–161.  
829 <https://doi.org/10.1093/molbev/msu285>
- 830 Krogerus, K., Arvas, M., De Chiara, M., Magalhães, F., Mattinen, L., Oja, M., Vidgren, V.,

- 831 Yue, J. X., Liti, G., & Gibson, B. (2016). Ploidy influences the functional attributes of  
832 de novo lager yeast hybrids. *Applied Microbiology and Biotechnology*, *100*(16), 7203–  
833 7222. <https://doi.org/10.1007/s00253-016-7588-3>
- 834 Krogerus, K., Holmström, S., & Gibson, B. (2018). Enhanced Wort Fermentation with De  
835 Novo Lager Hybrids. *Applied and Environmental Microbiology*, *84*(4), 1–20.  
836 <https://doi.org/10.1128/AEM.02302-17>
- 837 Krogerus, K., Magalhães, F., Vidgren, V., & Gibson, B. (2015). New lager yeast strains  
838 generated by interspecific hybridization. *Journal of Industrial Microbiology and*  
839 *Biotechnology*, *42*(5), 769–778. <https://doi.org/10.1007/s10295-015-1597-6>
- 840 Krogerus, K., Preiss, R., & Gibson, B. (2018). A unique *saccharomyces cerevisiae*  
841 *saccharomyces uvarum* hybrid isolated from norwegian farmhouse beer:  
842 Characterization and reconstruction. *Frontiers in Microbiology*, *9*(SEP), 1–15.  
843 <https://doi.org/10.3389/fmicb.2018.02253>
- 844 Langdon, Q. K., Peris, D., Baker, E. C. P., Ofulente, D. A., Nguyen, H. V., Bond, U.,  
845 Gonçalves, P., Sampaio, J. P., Libkind, D., & Hittinger, C. T. (2019). Fermentation  
846 innovation through complex hybridization of wild and domesticated yeasts. *Nature*  
847 *Ecology and Evolution*, *3*(11), 1576–1586. <https://doi.org/10.1038/s41559-019-0998-8>
- 848 Langdon, Q. K., Peris, D., Eizaguirre, J. I., Ofulente, D. A., Buh, K. V., Sylvester, K.,  
849 Jarzyna, M., Rodríguez, M. E., Lopes, C. A., Libkind, D., & Hittinger, C. T. (2020).  
850 Postglacial migration shaped the genomic diversity and global distribution of the wild  
851 ancestor of lager-brewing hybrids. *PLOS Genetics*, *16*(4), e1008680.  
852 <https://doi.org/10.1371/journal.pgen.1008680>
- 853 Langdon, Q. K., Peris, D., Kyle, B., & Hittinger, C. T. (2018). Sppider: A species  
854 identification tool to investigate hybrid genomes with high-throughput sequencing.  
855 *Molecular Biology and Evolution*, *35*(11), 2835–2849.  
856 <https://doi.org/10.1093/molbev/msy166>
- 857 Leadsham, J. E., & Gourelay, C. W. (2010). CAMP/PKA signaling balances respiratory

- 858 activity with mitochondria dependent apoptosis via transcriptional regulation. *BMC Cell*  
859 *Biology*, 11. <https://doi.org/10.1186/1471-2121-11-92>
- 860 Li, H., & Durbin, R. (2010). Fast and accurate long-read alignment with Burrows-Wheeler  
861 transform. *Bioinformatics*, 26(5), 589–595.  
862 <https://doi.org/10.1093/bioinformatics/btp698>
- 863 Li, H., Handsaker, B., Wysoker, A., Fennell, T., Ruan, J., Homer, N., Marth, G., Abecasis,  
864 G., & Durbin, R. (2009). The Sequence Alignment/Map format and SAMtools.  
865 *Bioinformatics*, 25(16), 2078–2079. <https://doi.org/10.1093/bioinformatics/btp352>
- 866 Liao, Y., Smyth, G. K., & Shi, W. (2014). FeatureCounts: An efficient general purpose  
867 program for assigning sequence reads to genomic features. *Bioinformatics*, 30(7), 923–  
868 930. <https://doi.org/10.1093/bioinformatics/btt656>
- 869 Libkind, D., Hittinger, C. T., Valerio, E., Goncalves, C., Dover, J., Johnston, M., Goncalves,  
870 P., & Sampaio, J. P. (2011). Microbe domestication and the identification of the wild  
871 genetic stock of lager-brewing yeast. *Proceedings of the National Academy of Sciences*,  
872 108(35), 14539–14544. <https://doi.org/10.1073/pnas.1105430108>
- 873 Love, M. I., Huber, W., & Anders, S. (2014). Moderated estimation of fold change and  
874 dispersion for RNA-seq data with DESeq2. *Genome Biology*, 15(12), 1–21.  
875 <https://doi.org/10.1186/s13059-014-0550-8>
- 876 Maddamsetti, R., Lenski, R. E., & Barrick, J. E. (2015). Adaptation, clonal interference, and  
877 frequency-dependent interactions in a long-term evolution experiment with escherichia  
878 coli. *Genetics*, 200(2), 619–631. <https://doi.org/10.1534/genetics.115.176677>
- 879 Mardones, W., Villarroel, C. A., Abarca, V., Urbina, K., Peña, T. A., Molinet, J., Nespolo,  
880 R. F., & Cubillos, F. A. (2021). Rapid selection response to ethanol in *Saccharomyces*  
881 *eubayanus* emulates the domestication process under brewing conditions. *Microbial*  
882 *Biotechnology*, 2, 1–18. <https://doi.org/10.1111/1751-7915.13803>
- 883 Mardones, W., Villarroel, C. A., Krogerus, K., Tapia, S. M., Urbina, K., Oporto, C. I.,  
884 Donnell, S. O., Minebois, R., Nespolo, R., Fischer, G., Querol, A., Gibson, B., &

- 885 Cubillos, F. A. (2020). Molecular profiling of beer wort fermentation diversity across  
886 natural *Saccharomyces eubayanus* isolates. *Microbial Biotechnology*, 1–14.  
887 <https://doi.org/10.1111/1751-7915.13545>
- 888 Martinez, C., Gac, S., Lavin, A., & Ganga, M. (2004). Genomic characterization of  
889 *Saccharomyces cerevisiae* strains isolated from wine-producing areas in South America.  
890 *Journal of Applied Microbiology*, 96(5), 1161–1168. [https://doi.org/10.1111/j.1365-](https://doi.org/10.1111/j.1365-2672.2004.02255.x)  
891 [2672.2004.02255.x](https://doi.org/10.1111/j.1365-2672.2004.02255.x)
- 892 Molinet, J., Eizaguirre, J. I., Quintrel, P., Bellora, N., Villarreal, C. A., Villarreal, P.,  
893 Benavides-Parra, J., Nespolo, R. F., Libkind, D., & Cubillos, F. A. (2022). Natural  
894 Variation in Diauxic Shift between Patagonian *Saccharomyces eubayanus* Strains.  
895 *MSystems*, 7(6). <https://doi.org/10.1128/msystems.00640-22>
- 896 Molinet, J., Urbina, K., Villegas, C., Abarca, V., Oporto, C. I., Villarreal, P., Villarreal, C.  
897 A., Salinas, F., Nespolo, R. F., & Cubillos, F. A. (2022). A *Saccharomyces eubayanus*  
898 haploid resource for research studies. *Scientific Reports*, 12(1), 5976.  
899 <https://doi.org/10.1038/s41598-022-10048-8>
- 900 Nespolo, R. F., Villarreal, C. A., Oporto, C. I., Tapia, S. M., Vega-Macaya, F., Urbina, K.,  
901 De Chiara, M., Mozzachiodi, S., Mikhalev, E., Thompson, D., Larrondo, L. F., Saenz-  
902 Agudelo, P., Liti, G., & Cubillos, F. A. (2020). An Out-of-Patagonia migration explains  
903 the worldwide diversity and distribution of *Saccharomyces eubayanus* lineages. *PLoS*  
904 *Genetics*, 16(5), e1008777. <https://doi.org/10.1371/journal.pgen.1008777>
- 905 Nikulin, J., Krogerus, K., & Gibson, B. (2018). Alternative *Saccharomyces* interspecies  
906 hybrid combinations and their potential for low-temperature wort fermentation. *Yeast*,  
907 35(1), 113–127. <https://doi.org/10.1002/yea.3246>
- 908 Okuno, M., Kajitani, R., Ryusui, R., Morimoto, H., Kodama, Y., & Itoh, T. (2015). Next-  
909 generation sequencing analysis of lager brewing yeast strains reveals the evolutionary  
910 history of interspecies hybridization. *DNA Research*, 23(1), 67–80.  
911 <https://doi.org/10.1093/dnares/dsv037>

- 912 Payen, C., & Dunham, M. J. (2016). Experimental Evolution and Resequencing Analysis of  
913 Yeast. In *Yeast Functional Genomics: Methods and Protocols* (Vol. 1361, pp. 361–374).  
914 [https://doi.org/10.1007/978-1-4939-3079-1\\_20](https://doi.org/10.1007/978-1-4939-3079-1_20)
- 915 Pockrandt, C., Alzamel, M., Iliopoulos, C. S., & Reinert, K. (2020). GenMap: Ultra-fast  
916 computation of genome mappability. *Bioinformatics*, *36*(12), 3687–3692.  
917 <https://doi.org/10.1093/bioinformatics/btaa222>
- 918 Quinlan, A. R., & Hall, I. M. (2010). BEDTools: A flexible suite of utilities for comparing  
919 genomic features. *Bioinformatics*, *26*(6), 841–842.  
920 <https://doi.org/10.1093/bioinformatics/btq033>
- 921 Ramakrishnan, V., Theodoris, G., & Bisson, L. F. (2007). Loss of IRA2 suppresses the  
922 growth defect on low glucose caused by the snf3 mutation in *Saccharomyces cerevisiae*.  
923 *FEMS Yeast Research*, *7*(1), 67–77. <https://doi.org/10.1111/j.1567-1364.2006.00159.x>
- 924 Rieseberg, L. H., Raymond, O., Rosenthal, D. M., Lai, Z., Livingstone, K., Nakazato, T.,  
925 Durphy, J. L., Schwarzbach, A. E., Donovan, L. A., & Lexer, C. (2003). Major  
926 ecological transitions in wild sunflowers facilitated by hybridization. *Science*,  
927 *301*(5637), 1211–1216. <https://doi.org/10.1126/science.1086949>
- 928 Santangelo, G. M. (2006). Glucose Signaling in *Saccharomyces cerevisiae*. *Microbiology*  
929 *and Molecular Biology Reviews*, *70*(1), 253–282.  
930 <https://doi.org/10.1128/mubr.70.1.253-282.2006>
- 931 Seehausen, O. (2004). Hybridization and adaptive radiation. *Trends in Ecology & Evolution*,  
932 *19*(4), 198–207. <https://doi.org/10.1016/j.tree.2004.01.003>
- 933 Sipiczki, M. (2018). Interspecies hybridisation and genome chimerisation in *Saccharomyces*:  
934 Combining of gene pools of species and its biotechnological perspectives. *Frontiers in*  
935 *Microbiology*, *9*(DEC), 1–20. <https://doi.org/10.3389/fmicb.2018.03071>
- 936 Steensels, J., Gallone, B., & Verstrepen, K. J. (2021). Interspecific hybridization as a driver  
937 of fungal evolution and adaptation. *Nature Reviews Microbiology*, *0123456789*.  
938 <https://doi.org/10.1038/s41579-021-00537-4>

- 939 Steensels, J., Gallone, B., Voordeckers, K., & Verstrepen, K. J. (2019). Domestication of  
940 Industrial Microbes. *Current Biology*, 29(10), R381–R393.  
941 <https://doi.org/10.1016/j.cub.2019.04.025>
- 942 Steensels, J., Snoek, T., Meersman, E., Nicolino, M. P., Voordeckers, K., & Verstrepen, K.  
943 J. (2014). Improving industrial yeast strains: exploiting natural and artificial diversity.  
944 *FEMS Microbiology Reviews*, 38(5), 947–995. [https://doi.org/10.1111/1574-](https://doi.org/10.1111/1574-6976.12073)  
945 [6976.12073](https://doi.org/10.1111/1574-6976.12073)
- 946 Stelkens, R. B., Brockhurst, M. A., Hurst, G. D. D., Miller, E. L., & Greig, D. (2014). The  
947 effect of hybrid transgression on environmental tolerance in experimental yeast crosses.  
948 *Journal of Evolutionary Biology*, 27(11), 2507–2519. <https://doi.org/10.1111/jeb.12494>
- 949 Stelkens, R., & Bendixsen, D. P. (2022). The evolutionary and ecological potential of yeast  
950 hybrids. *Current Opinion in Genetics & Development*, 76, 101958.  
951 <https://doi.org/10.1016/j.gde.2022.101958>
- 952 Stelkens, R., & Seehausen, O. (2009). GENETIC DISTANCE BETWEEN SPECIES  
953 PREDICTS NOVEL TRAIT EXPRESSION IN THEIR HYBRIDS. *Evolution*, 63(4),  
954 884–897. <https://doi.org/10.1111/j.1558-5646.2008.00599.x>
- 955 Talevich, E., Shain, A. H., Botton, T., & Bastian, B. C. (2016). CNVkit: Genome-Wide Copy  
956 Number Detection and Visualization from Targeted DNA Sequencing. *PLOS*  
957 *Computational Biology*, 12(4), e1004873. <https://doi.org/10.1371/journal.pcbi.1004873>
- 958 Ulery, T. L., Jang, S. H., & Jaehning, J. A. (1994). Glucose repression of yeast mitochondrial  
959 transcription: kinetics of derepression and role of nuclear genes. *Molecular and Cellular*  
960 *Biology*, 14(2), 1160–1170. <https://doi.org/10.1128/mcb.14.2.1160>
- 961 Urbina, K., Villarreal, P., Nespolo, R. F., Salazar, R., Santander, R., & Cubillos, F. A. (2020).  
962 Volatile compound screening using HS-SPME-GC/MS on saccharomyces eubayanus  
963 strains under low-temperature pilsner wort fermentation. *Microorganisms*, 8(5), 1–19.  
964 <https://doi.org/10.3390/microorganisms8050755>
- 965 Vagnoli, P., & Bisson, L. F. (1998). The SKS1 gene of *Saccharomyces cerevisiae* is required

- 966 for long-term adaptation of *snf3* null strains to low glucose. *Yeast*, *14*(4), 359–369.  
967 [https://doi.org/10.1002/\(sici\)1097-0061\(19980315\)14:4<359::aid-yea227>3.0.co;2-](https://doi.org/10.1002/(sici)1097-0061(19980315)14:4<359::aid-yea227>3.0.co;2-)  
968 %23
- 969 Venegas, C. A., Saona, L. A., Urbina, K., Quintrel, P., Peña, T. A., Mardones, W., &  
970 Cubillos, F. A. (2023). Addition of *Saccharomyces eubayanus* to SCOBY fermentations  
971 modulates the chemical and volatile compound profiles in kombucha. *Food*  
972 *Microbiology*, *116*(August). <https://doi.org/10.1016/j.fm.2023.104357>
- 973 Walker, G. M., & Basso, T. O. (2019). Mitigating stress in industrial yeasts. *Fungal Biology*.  
974 <https://doi.org/10.1016/j.funbio.2019.10.010>
- 975 Warringer, J., & Blomberg, A. (2003). Automated screening in environmental arrays allows  
976 analysis of quantitative phenotypic profiles in *Saccharomyces cerevisiae*. *Yeast*, *20*(1),  
977 53–67. <https://doi.org/10.1002/yea.931>
- 978 White, C., & Zainasheff, J. (2010). *Yeast: The Practical Guide to Beer Fermentation*.  
979 Brewers Publications.
- 980 Yue, J. X., Li, J., Aigrain, L., Hallin, J., Persson, K., Oliver, K., Bergström, A., Coupland,  
981 P., Warringer, J., Lagomarsino, M. C., Fischer, G., Durbin, R., & Liti, G. (2017).  
982 Contrasting evolutionary genome dynamics between domesticated and wild yeasts.  
983 *Nature Genetics*, *49*(6), 913–924. <https://doi.org/10.1038/ng.3847>
- 984 Zahn-Zabal, M., Dessimoz, C., & Glover, N. M. (2020). Identifying orthologs with OMA: A  
985 primer. *F1000Research*, *9*. <https://doi.org/10.12688/f1000research.21508.1>
- 986 Zörgö, E., Gjuvsland, A., Cubillos, F. A., Louis, E. J., Liti, G., Blomberg, A., Omholt, S. W.,  
987 & Warringer, J. (2012). Life history shapes trait heredity by accumulation of loss-of-  
988 function alleles in yeast. *Molecular Biology and Evolution*, *29*(7), 1781–1789.  
989 <https://doi.org/10.1093/molbev/mss019>
- 990 Zwietering M, H., Jongenburger I, L., Rombouts, F, M., & Van Riet, K. (1990). Modeling of  
991 the bacterial growth curve. *Applied and Environmental Microbiology*, *56*(6), 1875–  
992 1881.



993 **Figure Legends**

994 **Figure 1. Phenotypic characterization of interspecific F1 hybrids.** A) Hierarchically  
995 clustered heatmap of phenotypic diversity of 31 interspecific hybrids strains under  
996 microculture conditions. Phenotypic values are calculated as normalized z-scores. (B)  
997 Principal component analysis (PCA) using the maximum specific growth rates under six  
998 microculture growth conditions, together with the distribution of hybrid strains. Arrows  
999 depict the different environmental conditions. (C) Best-parent heterosis in the 31 interspecific  
1000 hybrids evaluated under microculture conditions in triplicates. (D) Fermentation capacity for  
1001 the 31 interspecific hybrids and parental strains at 12 °C. Plotted values correspond to mean  
1002 values of three independent replicates for each hybrid. Asterisk indicates different levels of  
1003 significance compared to the commercial strain W34/70 (Student t-test; \*\*\*  $p \leq 0.001$  and  
1004 \*\*\*\*  $p \leq 0.0001$ ). (E) Best-parent heterosis in the 31 interspecific hybrids evaluated under  
1005 fermentation conditions at 12 °C.

1006 **Figure 2. Fitness of evolved lines under microcultures and fermentation conditions.** (A)  
1007 Mean relative fitness (maximum  $OD_{600nm}$ ) of evolved lines after 250 generations under  
1008 microculture conditions. Evolved lines were evaluated in the same medium where they were  
1009 evolved (M or T medium). (B) Comparison of mean relative fitness (maximum  $OD_{600nm}$ )  
1010 shown in (A) between evolved lines from hybrids generated at 12 °C vs 20 °C. (C) Mean  
1011 relative fitness (maximum  $CO_2$  loss) of evolved lines after 250 generation under fermentation  
1012 conditions at 12 °C. (D) Comparison of mean relative fitness (maximum  $CO_2$  loss) shown in  
1013 (C) between evolved lines from hybrids generated at 12 °C vs 20 °C. (E) Maltotriose uptake  
1014 of evolved hybrid lines in maltose (M) and maltose/maltotriose (T), relative to the  
1015 commercial Lager strain W34/70. Ancestral hybrids are shown in grey, cold-generated and



1016 warm-generated hybrid lines are shown in blue and red, respectively. (F) Fermentative  
1017 capacity of evolved individuals relative to the commercial Lager strain W34/70 grouped  
1018 according to the environmental condition used during experimental evolution and  
1019 hybridization temperature to generate the ancestral hybrid. Plotted values correspond to the  
1020 mean of three independent biological replicates of each evolved line or strain. Asterisk  
1021 represents different levels of significance (Students t-test, \*  $p \leq 0.05$ , \*\*  $p \leq 0.01$ , \*\*\*  $p \leq$   
1022  $0.001$ , \*\*\*\*  $p \leq 0.0001$ , ns not significant).

1023 **Figure 3. Fermentation performance of evolved hybrid individuals.** (A) Maximum CO<sub>2</sub>  
1024 loss (g/L) for three different isolated genotypes (C1-C3) from evolved lines H3-4 and H4-1,  
1025 ancestral hybrids (H3-A and H4-A) and commercial lager strain (W34/70). (B) Ethanol  
1026 production (% v/v) for strains evaluated in (A). (C) Hierarchically clustered heatmap of  
1027 volatile compounds production for strains evaluated in (A). Phenotypic values are calculated  
1028 as normalized z-scores. For (A) and (B), plotted values correspond to the mean of three  
1029 independent replicates. The (\*) represents different levels of significance between hybrids  
1030 and commercial lager strain (Student t-test, \*\*  $p < 0.01$ , \*\*\*\*  $p < 0.0001$ ).

1031 **Figure 4. Genomic analysis of evolved hybrids.** (A) Total number of *de novo* SNPs in the  
1032 H3-E and H4-E hybrids. (B) SNP present in the *IRA2* gene in the *S. cerevisiae* sub-genome  
1033 in the H3-E hybrid. (C) Maximum OD<sub>600nm</sub> of *ira2Δ<sup>Sc</sup>* mutant strains under microculture  
1034 conditions. Mutant and wild-type strains were evaluated in the T medium. (D) CO<sub>2</sub> loss  
1035 kinetics for *ira2Δ<sup>Sc</sup>* mutant and wild-type strains. (E) Maltotriose uptake (%) for strains  
1036 evaluated in (D). For (C), (D) and (E), plotted values correspond to the mean of four  
1037 independent replicates. The (\*) represents different levels of significance between mutant  
1038 and wild-type strains (Student t-test, \*  $p < 0.05$ , \*\*\*  $p < 0.001$ , \*\*\*\*  $p < 0.0001$ ).

1039 **Figure 5. Copy number variation and differential gene expression analysis.** (A) Copy  
1040 number variations (CNVs) between H3-E and H4-E hybrids relative to their ancestral hybrids  
1041 found in *S. cerevisiae* chromosome 7. Coding genes located within bins showing CNV calls  
1042 higher than 1 copy (yellow rectangles) are shown. (B) Volcano plot showing differential  
1043 expressed genes (DEGs) between H3-E and H3-A hybrids. The red and blue dots represent  
1044 up-regulated and down-regulated genes in the H3-E hybrids, respectively. (C) Orthologous  
1045 genes showing an interaction between allelic expression and experimental evolution. (D)  
1046 Model depicting genes exhibiting mutations after the experimental evolution assay  
1047 (highlighted in orange) and involved in pathways related to the detection, regulation, uptake,  
1048 and catabolism of maltotriose. Phosphorylation is indicated in red. Green depicts a glucose  
1049 sensing protein, while proteins in blue highlight transporters involved in sugar consumption.

#### 1050 **Supplementary information**

1051 **Figure S1. Generation of interspecific *S. cerevisiae* x *S. eubayanus* hybrids.** Experimental  
1052 procedure designed to generate and identify interspecific hybrids at two different  
1053 temperatures (12 and 20°C).

1054 **Figure S2. Phenotypic characterization of *S. cerevisiae* parental strains.** (A)  
1055 Fermentation performance of 15 *S. cerevisiae* strains. (B) Maximum OD reached of growth  
1056 curves in maltotriose 2% under microculture conditions (C) Maltotriose uptake after growth  
1057 in maltotriose 2% under microculture conditions. Plotted values correspond to three  
1058 biological replicates. The (\*) represents different levels of significance between the  
1059 phenotype of haploid strains and their respective parental strain (t-test; \* $p \leq 0.05$ , \*\* $p \leq 0.01$ ,  
1060 \*\*\* $p \leq 0.001$ , \*\*\*\* $p \leq 0.0001$  and ns: non-significant).

1061 **Figure S3. Fermentative capacity at 12 °C of each hybrid.** Each plot represents a different  
1062 cross. The (\*) represents different levels of significance between the phenotype of hybrids  
1063 and their respective parental strain (t-test; \* $p \leq 0.05$ , \*\* $p \leq 0.01$ , \*\*\* $p \leq 0.001$ , \*\*\*\* $p \leq$   
1064 0.0001).

1065 **Figure S4. Fitness comparison of evolved lines after 250 generations.** (A) Mean relative  
1066 fitness (growth rate) of evolved lines after 250 generation under microculture conditions.  
1067 Evolved lines were evaluated in the same medium where they were evolved (M o T medium).  
1068 (B) Mean relative fitness (growth rate) comparison between evolved lines from hybrids  
1069 generated at 12 and 20 °C. Plotted values correspond to the mean of three independent  
1070 replicates of each evolved lines. The (\*) represents different levels of significance between  
1071 evolved lines and unevolved hybrid in (A) and from hybrids generated at 12 °C vs 20 °C in  
1072 (B) (Students t-test, \*  $p < 0.05$ , \*\*  $p < 0.01$ , ns not significant).

1073 **Figure S5. Fitness dynamics of evolved lines in maltose and maltose with maltotriose.**  
1074 (A) Mean relative fitness (growth rate and OD) of replicate population in 2% maltose. (B)  
1075 Mean relative fitness (growth rate and OD) of replicate population in 1% maltose and 1%  
1076 maltotriose. Plotted values correspond to the mean of three independent replicates of each  
1077 evolved line.

1078 **Figure S6. Fitness dynamics of evolved lines in maltose and maltose with maltotriose**  
1079 **under fermentation condition.** (A) Mean relative fitness (maximum CO<sub>2</sub> loss) of replicate  
1080 population in 2% maltose. (B) Mean relative fitness (maximum CO<sub>2</sub> loss) of replicate  
1081 population in 1% maltose and 1% maltotriose. Plotted values correspond to the mean of three  
1082 independent replicates of each evolved line.

1083 **Figure S7. Fermentative capacity of evolved individuals.** Fermentative capacity of  
1084 evolved individuals relative to the commercial lager strain W34/70. Plotted values  
1085 correspond to the mean of three independent replicates of each individual. The (\*) represents  
1086 different levels of significance between strains and commercial lager strain (Students t-test,  
1087 \*  $p < 0.05$ , \*\*  $p < 0.01$ , \*\*\*  $p < 0.001$ ).

1088 **Figure S8. GO term enrichment for genes with *de novo* mutations.** (A) Enriched GO  
1089 terms identified in genes with *de novo* mutations in H3-E. (B) Enriched GO terms identified  
1090 in genes with *de novo* mutations in H4-E.

1091 **Figure S9. Dynamics of molecular evolution.** Allele frequencies over time in H3-A line  
1092 evolved in T medium. In different colours are highlighted SNPs in the genes *IRA2*, *MAL32*  
1093 and *SNF3*.

#### 1094 **Table Legends**

1095 **Table S1.** (A) Strains used in this study. (B) Primers used in this study.

1096 **Table S2.** (A) Phenotypic characterization of the *S. cerevisiae* strains under fermentation  
1097 conditions (maximum CO<sub>2</sub> loss). (B) Statistical analysis of fermentative capacity of *S.*  
1098 *cerevisiae* strains. (C) Sporulation efficiency and spore viability for *S. cerevisiae* and *S.*  
1099 *eubayanus* strains.

1100 **Table S3.** (A) Phenotypic characterization of the 31 interspecific hybrids and parental strains  
1101 under microculture conditions. (B) Statistical analysis of phenotypes under microculture  
1102 conditions. (C) Best-parent heterosis in the 31 interspecific hybrids evaluated under

1103 microculture conditions. (D) Mid-parent heterosis in the 31 interspecific hybrids evaluated  
1104 under microculture conditions.

1105 **Tables S4.** (A) Fermentation capacity (maximum CO<sub>2</sub> loss) of hybrids in 12 °Brix wort at  
1106 12 °C. (B) Statistical analysis of fermentative capacity of hybrids at 12 °C. (C) Best-parent  
1107 heterosis for fermentative capacity. (D) Mid-parent heterosis for fermentative capacity. (E)  
1108 Sugar consumption and ethanol production of four interspecific hybrids and parental strains.  
1109 (D) Statistical analysis of maltotriose uptake and ethanol production.

1110 **Table S5.** (A) Mean relative fitness (growth rate and OD) and statistical analysis of each of  
1111 the evolved lines in maltose and maltose/maltotriose relative to unevolved hybrid. (B) Mean  
1112 relative fitness (growth rate and OD) and statistical analysis of evolved hybrids in maltose  
1113 and maltose/maltotriose relative to unevolved hybrid. (C) SNPs identified in the *COX3* gen.  
1114 (D) Identity matrix derived from *COX3* gen multiple alignment.

1115 **Table S6.** (A) Mean relative fitness and statistical analysis for maximum CO<sub>2</sub> loss of each  
1116 of the evolved lines in maltose and maltose/maltotriose relative to unevolved hybrid. (B)  
1117 Mean relative fitness and statistical analysis for maximum CO<sub>2</sub> loss of evolved hybrids in  
1118 maltose and maltose/maltotriose relative to unevolved hybrid. (C) Maltotriose uptake and  
1119 statistical analysis of evolved lines in maltose and maltose/maltotriose relative to commercial  
1120 Lager strain W34/70. (D) Mean relative fitness and statistical analysis for maximum CO<sub>2</sub>  
1121 loss of evolved lines in maltose and maltose/maltotriose relative to commercial Lager strain  
1122 W34/70.

1123 **Table S7.** (A) Fermentative capacity, maltotriose uptake and ethanol production of evolved  
1124 individuals of H3-A and H4-A hybrids. (B) Volatile compounds production of H3-4-C1 and  
1125 W34/70 in beer wort.

1126 **Table S8.** (A) Bioinformatics summary statistics. (B) Genomic contributions (%) from  
1127 parental strains in the H3-E and H4-E hybrids. (C) SnpEff analysis of the novel  
1128 polymorphisms in H3-E and H4-E. (D) CNV results comparing evolved hybrids with their  
1129 ancestral hybrid. Only CNVs with 1 or more copies are listed. (E) RNA-seq analysis between  
1130 H3-E and H3-A hybrids. (F) Enriched GO terms of hybrid genes showing differential  
1131 expression between ancestral and evolved hybrids. (G) Genes exhibiting Allele-Specific  
1132 Expression (ASE), with values approximating 1 indicating overexpression of *S. cerevisiae*  
1133 alleles, and values close to 0 representing overexpression of *S. eubayanus* alleles..

1134 **Table S9.** Fermentative capacity and maltotriose uptake of *ira2* mutants.